PONTIFICIA UNIVERSIDAD CATÓLICA DE PERÚ

FACULTAD DE CIENCIAS E INGENIERÍA

CUANTIFICACIÓN DE LA EROSIÓN HÍDRICA EN EL PERÚ Y LOS COSTOS AMBIENTALES ASOCIADOS

Tesis para obtener el grado de magister en Ingeniería Civil, presentada por:

ROSAS BARTURÉN, Miluska Anthuannet

Asesorada por:

PhD. GUTIERREZ LLANTOY, Ronald Roger

Lima, 3 de Marzo del 2016

Agradecimientos:

Deseo agradecer a Dios por darme la oportunidad de terminar mis estudios de posgrado, además agradezco a CONCYTEC como institución que fomenta la investigación en nuestro país y financia el desarrollo de jóvenes profesionales, finalmente agradezco a la Pontificia Universidad Católica del Perú por todos los conocimientos impartidos y por la orientación profesional para culminar exitosamente el trabajo de investigación.

TABLA DE CONTENIDOS

RESUMEN EJECUTIVO

Se presenta a la erosión de suelos como un problema latente alrededor del mundo, esta situación se agrava en los países en desarrollo por la falta de información actualizada, como es el caso del Perú. Por ello esta investigación tiene como objetivo plantear una metodología para cuantificar la tasa de erosión actual y futura a nivel nacional y escala de cuenca para así poder plantear lineamientos de regulación ante las pérdidas económicas que esta genera.

El **Capítulo 1** presenta la problemática, los objetivos y alcances de investigación. Además se detalla la metodología para llevar a cabo los fines propuestos, mostrando el producto del proceso de investigación (3 papers científicos).

El C**apítulo 2** presenta el primer paper titulado: *On a RUSLE-based methodology to estimate hydraulic erosion rates at country scale in developing countries*, que plantea una metodología para estimar la erosión de suelos a escala nacional ante un contexto de escases de información básica como ocurre en los países en desarrollo. Tiene como producto mapas de la tasa de erosión de suelos en el Perú para los años 1990, 2000 y 2010 a una resolución de 5km.

El **Capítulo 3** muestra el segundo paper cuyo título es*: Sediment yield changes in the Peruvian Andes for the year 2030*, cuyo objetivo es mostrar la significancia de la cantidad de sedimentos producidas en los Andes peruanos con una proyección al año 2030. Se evaluaron 2 escenarios adicionales, el primero que incluye el desarrollo de la actividad minera en el país y el segundo donde se presentan las áreas de protección ambiental.

El **Capítulo 4** está conformado por el tercer paper: *On the need of erosion control regulatory framework in Peru*, en el cual se detalla la importancia de una regulación en términos de erosión, basando esta afirmación en la pérdida económica inducida como fuente de contaminación no puntual. Tiene como casos de estudio la cuenca del río Santa y del río Jequetepeque. Esta estimación económica envuelve la pérdida de nutrientes y el costo por la eliminación de sedimentos en la cuenca.

CAPITULO 1: EL PROBLEMA DE INVESTIGACIÓN

1 Planteamiento del problema y justificación

La pérdida de suelos por causa de erosión hídrica es un problema que se agrava, especialmente en los países en desarrollo, debido a la falta de información actualizada, como es el caso del Perú. Los últimos estudios al respecto fueron realizados por el Instituto Nacional de Recursos Naturales (INRENA) en 1996 y solo proveen información cualitativa de los procesos erosivos, es así que este estudio tiene como objetivo cuantificar el riesgo de la erosión en el país y definir lineamientos preliminares para su control. En primer lugar se identificará la metodología que se adecua a las condiciones climáticas y a la disponibilidad de información para obtener resultados a escala regional y, subsecuentemente, de cuenca. Luego se cuantificará la tasa de erosión actual y proyectada, lo que permitirá realizar una estimación económica para así, plantear los lineamientos necesarios para su regulación.

2 Objetivos de la investigación

2.1 Objetivo general:

El objetivo general del proyecto es estimar y cuantificar la tasa de erosión hídrica en países en desarrollo, siendo Perú el caso de estudio, con el fin de desarrollar un marco de regulación.

2.2 Objetivos específicos:

- Estudiar las modelos aplicables a escala regional y a escala de cuenca.
- Estimar la tasa de erosión hídrica en nuestro país y realizar una proyección futura.
- Realizar una valoración económica de los costos inducidos por la erosión hídrica a escala de cuenca y diseñar preliminarmente los lineamientos para regulación en materia de control de erosión.

2.3 Alcances:

Se cuantificará el riesgo de erosión hídrica de suelos (no incluye erosión en bancos ni fallas masivas). Se identificará el/los modelo(s) adecuado(s) a las condiciones climáticas y a la data disponible para realizará una cuantificación a escala regional y a escala de cuencas (cuenca del río Santa). Finalmente, se plantearán los lineamientos para regular el control de la erosión en el país.

3 Metodología y plan de trabajo

A continuación se presentan las actividades para el desarrollo de la investigación:

1. Problemática y estado del arte

1.1Antecedentes de erosión de suelos a nivel nacional: Investigar a cerca de la problemática actual de la pérdida de suelos por la acción de la erosión hídrica. Recopilar información de estudios realizados en el país.

1.2Antecedentes de erosión de suelos a nivel internacional: Recopilación de información de modelos aplicados en otros países.

2. Metodología para la cuantificación de erosión.

2.1Recopilación de información nacional disponible: información tanto de entidades nacionales como internacionales. Incluye data meteorológica, uso de suelo, data geológica, información topográfica, etc.

2.2Detalle de los modelos existentes para la cuantificación de la erosión a escala regional (RUSLE) y a escala de cuenca (WEEP, SWAT y LISEM). Se recopilará información acerca de los datos de entrada, escalas aplicables, teoría del modelo y resultados obtenidos.

2.3Detalle de los modelos existentes de inferencia (proyección futura) entre ellos: modelo de regresión y modelo de transición de Markov.

3. Cuantificación de erosión hídrica de suelos en el país.

3.1Modelamiento de la erosión a escala regional: se aplicarán los modelos que se adecuen a nuestras condiciones climáticas y topográficas. Se realizará una estimación del riesgo de erosión actual y proyectada a nivel nacional.

3.2Modelamiento de la erosión a escala de cuenca: Se aplicarán los modelos adecuados a la cuenca del río Rímac. Se estimará el riesgo actual y proyectado.

4. Propuesta para la regulación de erosión en el país.

Se plantearán lineamientos y normativas para la regulación de la erosión hídrica de suelos, a partir del modelamiento realizado. Previamente se realizará una cuantificación económica se las perdidas inducidas por erosión de suelos.

5. Elaboración de papers.

Se presentarán dos (3) papers exponiendo el producto de la investigación, cuyos títulos serán: “On a RUSLE-based methodology to estimate hydraulic erosion rates at country scale in developing countries”, “Sediment yield changes in the Peruvian Andes for the year 2030” y “On the need of erosion control regulatory framework in Peru”.

CAPITULO 2:

On a RUSLE-based methodology to estimate hydraulic erosion rates at country scale in developing countries

Reviews in Environmental Science and Bio/Technology manuscript No.
(will be inserted by the editor)

A RUSLE-based method to estimate soil erosion rates at country scale in developing countries

Miluska A. Rosas · **Ronald R. Gutierrez**

Received: date / Accepted: date

Abstract This study proposes a RUSLE-based method to estimate soil erosion rates at country scale for developing countries, which commonly exhibit temporal and spatial limitations in ground-based measurements of the fundamental parameters describing such model. The method proposed herein mainly uses up-to-date publicly available datasets. Likewise, it elaborates on the preprocessing of such data, focuses on the *R* and *C* factor of the RUSLE model because they are critical parameters for the model in developing countries, and suggests the use of the sediment delivery ratio as a proxy parameter to validate the RUSLE model. The method is explained through a direct application to Peru, and subsequently erosion rate maps at 5-km resolution are obtained. Our results show that Peru is facing an steady increase of soil erosion rates (19 $mill\ ton/year$ for 1990, 26 $mill\ ton/year$ for 2000, and 41 $mill\ ton/year$ for 2010) which are mainly induced by changes in land use. It is expected that Peru keeps such trend because it is increasing its infrastructure portfolio and the areas devoted to concessions for the extractive industry, and its urban population is rapidly growing. Possibly, such is also the case in many developing countries. In the light of our results, we believe that the method has the potential to provide decision makers for an objective information to better manage soil resources in developing countries.

Keywords hydraulic soil erosion · sediment yield · data scarcity · RUSLE · land use change

1 Introduction

Hydraulic soil erosion usually displays complex interactions between geomorphological features and processes (e.g., rain splash erosion, sheetwash erosion, rill, interrill and gully erosion, mass movement, channel erosion [1]), and anthropological controls (e.g., increasing

M. A. Rosas
Pontificia Universidad Católica del Perú, Av. Universitaria 1801, San Miguel, Lima 32, Peru
Tel.: +511-626-4660
E-mail: miluska.rosas@pucp.pe

R. R. Gutierrez
Pontificia Universidad Católica del Perú, Av. Universitaria 1801, San Miguel, Lima 32, Peru
Tel.: +511-626-4660
E-mail: rgutierrezl@pucp.pe

population, deforestation, land cultivation, construction, uncontrolled grazing, among others). As a result, in many instances, fertile topsoil is removed [2] and/or sediments are transported over the landscape and water bodies [3]. Thus, hydraulic soil erosion is commonly associated to economic losses in several countries all around the world [4], and thereby represents a societal concern [5,6].

In the past decades many conceptual, empirical, and physically based soil erosion models have been developed. Empirical models (e.g., Watem-Sedem [7], AGNPS [8], SWAT [9]) are mainly based on field relations of statistical significance. They are based on the Revised Universal Soil Loss Equation (RUSLE) which has the capability to estimate sheetwash and rill erosion [10,11] and thus, is useful for identifying the sources of sediments and providing valuable information to catchment managers and decision makers [12].

Copious field, experimental and numerical modeling studies aimed to quantify hydraulic soil erosion rates (ERs) have been performed in developed countries [13,14], at plot, microcatchment, catchment (through sediment yield and budgeting work), country [15–17] and, global scale [18]. Notwithstanding these achievements, the understanding of the effects of scale in soil erosion observations is not clear yet [17].

Very few studies have addressed the quantification ERs in developing countries [2,19,20], probably because of the fact that they lack or face limitations on the availability of both spatial and temporal ground-based measurements and field relations being required to estimate ERs, and an appropriate erosion control regulatory framework. In this context, publicly available data from satellite sensors, which offer a unique global observational platform for managing land, water, agriculture, and ecosystem functions [21–23], and to which soil erosion is closely related, has the potential to provide fundamental information to estimate ERs in developing countries. Despite exhibiting such potential, however, it is still fare to state that the prospective social benefits of free available satellite data have not been fully achieved yet [23], and apparently, such is also the case of other global data sets (e.g., up-to-date datasets published by Japan Space System, FAO Land Water Division, World Soil Museum, etc.) that describe the fundamental parameters of the RUSLE model.

The objective of this research is two fold. Firstly, to propose a methodology to estimate ERs in developing countries by combining up-to-date global publicly available data from satellite measurements, global models (e.g., soil, land cover, deforestation, among others), and conventional ground-based source data managed by public local agencies; and secondly, to apply the proposed method to develop ER country scale maps for Peru. This country exhibits marked soil erosion spatial variability due to particular topographic and climate conditions induced by the tropical Andes which triggers convective storms in the arid highlands [24, 25], the Amazon rainforest which covers around 60% of its territory, the occurrence of severe rainstorms when El Niño Southern Oscillation hit the arid coastal area [26,27], and the fact that the Peruvian economy relies on its natural resources (i.e., mining, petroleum, gas) [28,29]. Likewise, global models suggest that Peru will face variations in precipitation patterns due to global warming [30]. Despite such critical aspects, to the best of our knowledge, no quantitative study of soil erosion exist in Peru, the last soil erosion country official map was published in 1996 and only provides qualitative information about the matter [31]. Moreover, past research have highlighted the fact that Peru exhibits limitations in the availability of climatological and hydrological data to estimate the variation of sediment yield (SY) and its relationship with ER and other factors [24,32].

This paper is organized as follows: section 2 describes the sources and evolution of the global and local basic data that RUSLE model requires, and elaborates on the methodology we propose. Section 3 presents the results and model validation, and finally, section 4 covers

the main conclusions and remarks.

2 Data and Method

2.1 Availability of global and local data sets

The RUSLE model allows for quantifying ERs for a variety of agricultural practices, soil types and climatic conditions, and therefore, meteorological, geological, topographical, and land cover information are required. In recent years, several remote sensing technology missions (e.g., Landsat and altimetry missions, hydrologic missions like Global Precipitation Measurement, NASA's Gravity Recovery and Climate Experiment mission, and NASA's anticipated Surface Water and Ocean Topography mission) have focused in measuring these environmental parameters [23]. In the last five years the measured data has markedly improved in terms of availability and resolution (see Table 1). Historic estimates of ER at country scale may be limited to back the year 1990 due to resolution limitations from satellite data and data scarcity from local agencies. Thus, for the case of Peru, ER was quantified for the years 1990, 2000, and 2010 and the input source data is presented in Table 1.

Table 1 Input data used to estimate Peruvian ER maps for the years 1990, 2000 and 2010

Item	Name	Source	Resolution	Year
A	Global Precipitation Climatology Project (GPCP) data [33]	NOAA	2.5°	1979
B	Tropical Rainfall Measuring Mission (TRMM) [34]	NASA	0.25°	1998
C	Rainfall data	Autoridad Nacional del Agua, ANA	Monthly	Varie
D	Sand, silt and clay content maps [35]	ISRIC - World Soil Information	1 km	2013
E	Organic carbon content map [35]	ISRIC - World Soil Information	1 km	2013
F	ASTER Digital Elevation Model [36]	Japan Space System and NASA	30 m	2009
G	Global Forest Canopy Height [37]	ORNL DAAC from NASA	1 km	2011
H	Global Land Use/Land Cover images (15 classes) [38]	USGS EROS Data Center	0.1°	1992
I	The Global Land Cover Facility (16 classes) [39]	MODIS Land Cover	0.25′	2001
J	Global Land Cover Share Database (10 classes) [40]	FAO, Land and Water Division	1km	2014
K	Ecological Peruvian map (shapefiles)	Oficina Nacional de Evaluacin de Recursos Naturales, ONERN		1997
L	Vegetative Cover Peruvian map (shapefiles)	Ministerio del Ambiente, MINAM		2010
M	Sediment load data, Gallito Ciego reservoir, Jequetepeque basin	Instituto Nacional de Recursos Naturales, INRENA	Monthly	Oct.
N	Sediment load data, Poechos reservoir, Chira basin	Autoridad Nacional del Agua, ANA	Annual	1976
O	Sediment load data, Condorcerro station, Santa basin	Chavimochic Special Project	Daily	1999

The Global Energy and Water Exchange program and the Tropical Rainfall Measuring Mission probably represent the most reliable sources of global and free available precipitation data. They were launched to quantify the distribution of global precipitation around the globe and estimate monthly rainfall in global coverage to validate global climate models. The former (item A in table 1) provides data from January 1979 through the present [33] and combines satellite IR data from Geostationary imagers, sounding data from the TIROS Operational Vertical Sounder and the Atmospheric Infrared sounder, microwave imager data from the Special Sensor Microwave Imagers, and surface rain gage data [41,42]. The latter (item B in table 1) is a joint mission between NASA and the Japan Aerospace Exploration and measured rainfall and energy exchange of tropical and subtropical regions of the world

since 1997 [34]. On the other hand, precipitation data from local meteorological agencies requires having at least a ten-year data length of anticipation to the year of interest [43]. For the case of Peru, monthly rainfall data (item C in Table 1) was collected from 151, 132, and 76 meteorological stations for the years 1990, 2000, and 2010, respectively. In others countries, meteorological data might be collected from local agencies, e.g. Servicio Meteorologico Nacional in Argentina [44], Malaysian Meteorological Department in Malaysia [20], Instituto Nacional de Recursos Hidraulicos in Dominican Republic [45] and Islamic republic of Iran meteorological organization [19]. Commonly, in developing countries, the lack of available and continuous rainfall data collection is evident, such is the case of Peru, where information has been defined as uncertain, incomplete and not representative on spatial distribution [46].

Likewise, based on validated satellite data, soil property data (items D and E) have been generated by ISRIC - World Soil Information as a result of international collaboration among the University of Sao Paulo, SOTER China, AGR Canada, INEGI Mexico, etc. to obtain soil information maps at 1-km resolution. This source has noncommercial purposes and the initiatives to serve as a link between global and local soil mapping [35].

Some digital elevation models for the entire globe have been produced to provide accessibility of high quality elevation data. One of the most up to date information is the ASTER Global Digital Elevation Model (item F in table 1) which was released by NASA and the Ministry of Economy, Trade and Industry of Japan in June 2009, and covers 99% of Earth's surface [36]. This data is available in both ArcInfo ASCII and GeoTiff format to facilitate its access.

Land cover data has mainly been developed by local agencies (e.g. Instituto Nacional de Tecnologia Agropecuaria in Argentina [44], Agriculture Department in Malaysia [20] Secretaria de Estado de Medio Ambiente y Recursos Naturales in Dominican Republic [45], Ministerio del Ambiente in Peru, etc.); however, such information is not publicly available in some developing countries as they try to benefit by selling their data [47]. Therefore, the Global Land Cover Share Database launched by FAO (item J in Table 1) is recommended as the main information source to estimate the spatial and temporal variability of the land cover. This stems on the fact that, in contrast with the other sources (i.e., items H and I in Table 1), this one represents the most up-to-date available data and provides for valuable information about the dominant land cover class and its density in each cell (i.e. a pixel). This variable might be the most time sensible factor in Peru, because as a developing country, it is rapidly increasing its volume of infrastructure, and the areas devoted to concessions for the logging, mining, gas and oil industries, and therefore, significant changes in land use are expected in the short and medium terms [29, 24].

2.2 Model structure

2.2.1 Data preprocessing

Satellite data processing, in many instances, involves filling data gaps, standardizing parameters and interpolating [48], and depending on data characteristics and resolution, multiple regression, correlation coefficient, mean bias error, and root-mean-square error methods are commonly used to validate satellite data[18, 49, 50]. ERs quantification requires analyzing two groups of datasets, namely: rainfall (i.e., ground station, and satellite data) and land cover.

For the case of Peru, rainfall data from ground stations was spatially interpolated by using

Kriging and a Gaussian semi-variogram model [51]. Thus, the resulting raster resolution was 0.25°, which is equal to the TRMM resolution (Table 1). Subsequently, rainfall data from satellite data was validated with local information and evaluated in regions with similar climatic patterns (i.e. Coastal, Andean, and Amazonian areas). The correlation coefficient (r) and the mean bias error (MBE) were estimated in each region in monthly steps. Commonly, if $r \geqslant 0.5$ and $MBE < 0.5$, the data is considered to be reliable in relative terms [50,49]. Figure 1 shows that the 85% of the validated stations located in the coastal area have an acceptable $r > 0.5$ and approximately 60% of them have a $MBE < 0.5$. Similarly, in the Andean area, 50% of the stations have a $r > 0.5$ and the majority of them ($> 90\%$) present acceptable MBE. Similarly, in the Amazonian area, the majority of the stations ($> 90\%$) present acceptable r and MBE.

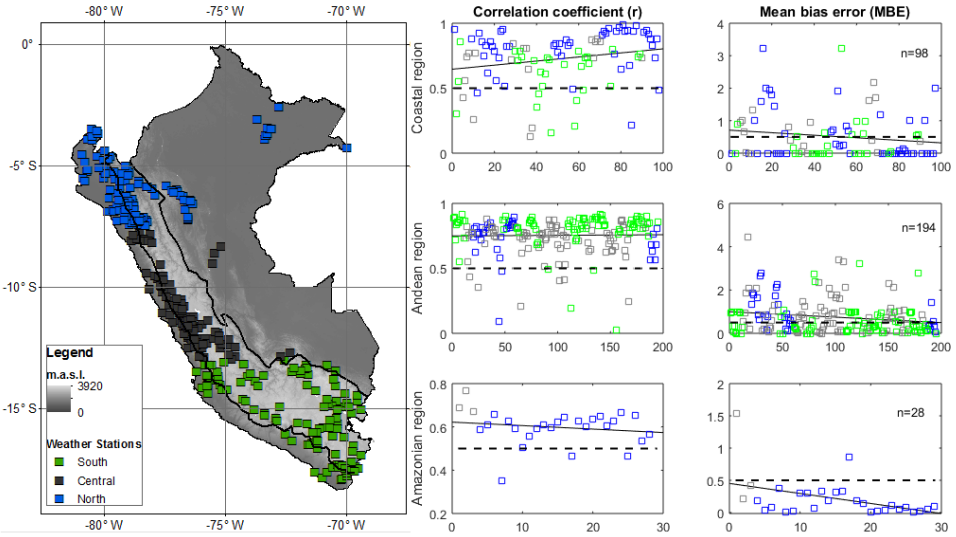

Fig. 1 Satellite rainfall validation analysis. The country was divided in three geographical regions, namely: Coastal (western), Andean (central), and Amazonian (eastern) regions. n represents the number of meteorological stations being analyzed in each region. Blue, black and green circle marks represent the stations located in the Northern, Central and Southern Peru, respectively. Dotted lines represent the acceptable threshold of MBE (< 0.5) and r ($\geqslant 0.5$).

For the case of Peru, land cover information, which comprises global land cover databases (items H through L in Table 1), was re-categorized in order to standardize the number of classes based on the Global Land Cover Share Database (10-class land cover). This operation is probably necessary for most of the developing countries due to the prevailing resolution of the free available data.

2.2.2 The RUSLE model

Several studies have addressed the definition of the RUSLE model and the variables that define it (Eq. 1); however, most of these studies do not focus on identifying the sensibility

of the model in contexts where basic data is limited. The RUSLE model is mathematically defined by Eq. 1.

$$A = R \times K \times L \times S \times C \times P \tag{1}$$

where A is the annual soil erosion ($t\ ha^{-1}\ year^{-1}$); R is the rainfall erosivity factor which is expressed in $MJ\ mm\ ha^{-1}\ h^{-1}\ year^{-1}$; K is the soil erodibility factor ($t\ h\ MJ^{-1}\ mm^{-1}$); L is the slope length factor; S is the slope steepness factor; C is the cover management factor; and P is the conservation supporting practices factor (L, S, C and P are dimensionless). These variables can be categorized as static (i.e., features that remain constant in time such as K, L and S) and dynamic (i.e., time sensitive variables such as R, C and P). The later variables deserve special attention as they are scarce or inexistent in developing countries.

To estimate the R factor (Eq. 2), past studies (e.g. [11]) recommend using the Fournier index (F) in regions where information scarcity is an issue.

$$F = \frac{1}{N}\sum_{j=1}^{N}\left(\sum_{i=1}^{12}\frac{p_i^2}{p}\right) \tag{2}$$

In Eq. 2, p_i is the monthly rainfall, p is the mean annual rainfall and N is the number of years being evaluated. To obtain the R factor, we applied both the Arnoldus (R_A, Eq. 3) and the Renard and Freimund (R_{RF}, Eq.4). These relationships were developed for different geographical contexts [11], however it has been commonly used to estimate R factor in contexts where no detailed climate data exists [52].

$$R_A = 0.264F^{1.50} \tag{3}$$

$$R_{RF} = 0.07397F^{1.847} \tag{4}$$

Thus, for the case of Peru, two sets of scenarios were evaluated, the first one using R_A in the whole country, and the second one using R_{RF} solely in the coastal region because it is only applicable to regions exhibiting low precipitation rates [11]. Such is the case of the Peruvian coastal region that is classified as $Ea23$ and $Aa22$ arid land areas, based on the Meigs classification scheme [53].

In developing countries, the K factor, which is mathematically defined by Eq. 5, can be obtained by using the Wishmer and Smith equation [54]. The K factor depends upon the soil organic matter content (OM), particle size parameter (M), soil structure (s) and permeability (p). In this way, M is estimated by multiplying the (% silt + % sand) by ($100\%clay$), and later a factor of 1.8 is applied to obtain OM from organic carbon content data (item E in Table 1) as suggested by [55]. This procedure was applied for Peru.

$$K = 10^{-2}[2.1\times10^{-4}(12-OM)M1.14 + 3.25(s-2) + 2.5(p-3)]/7.59 \tag{5}$$

The L (Eq. 6 through 8) and S (Eq. 9) factors are typically obtained from a Digital Elevation Model. In the aforementioned equations, θ represents the slope angle.

$$L = \left(\frac{\lambda}{22.13}\right)^{m} \tag{6}$$

$$m = \frac{\beta}{1+\beta} \tag{7}$$

$$\beta = \frac{\sin\theta/0.0896}{3\times(\sin\theta)^{0.8}+0.56} \tag{8}$$

$$S = \begin{cases} 10.8\sin\theta + 0.03, & if\ \tan\theta < 0.09 \\ 16.8\sin\theta - 0.5, & if\ \tan\theta \geq 0.09 \end{cases} \tag{9}$$

The C factor is based on descriptions of cropping and cover management practices and their influence on soil loss [54], and is mathematically defined by Eq. 10. This factor is determined by the prior-land use subfactor (PLU), the canopy-cover subfactor (CC), the surface-cover subfactor (SC), the surface-roughness subfactor (SR), and the soil moisture subfactor (SM). Table 2 presents commonly used values to estimate this spatial sensitive factor, although for more details on the quantification of the aforementioned subfactors, the reader is kindly referred to [54].

$$C = PLU \times CC \times SC \times SR \times SM \tag{10}$$

Table 2 Subfactors detail from C factor

$\mathbf{C} = \mathbf{PLU} \times \mathbf{CC} \times \mathbf{SC} \times \mathbf{SR} \times \mathbf{SM}$ [54]	
$PLU = C_f \times C_b \times exp(-c_{ur} \times B_{ur})$	C_f :surface-soil consolidation factor $C_f = 0.45$ (cropland areas) $C_f = 1$ (all the land cover types) C_b : effectiveness of subsurface residue in consolidation B_{ur} : mass density of live and deat roots c_{ur} : calibration coefficients of the subsuface residues
$CC = 1 - F_c \times exp(-0.1 \times H)$	F_c : fraction of land surface covered by canopy H : canopy height
$SC = exp\left\{ -b \times S_p \times \left(\frac{0.24}{R_u}\right) \right\}$	b : empirical coefficient $b = 0.035$ (erosion in cropland areas) $b = 0.025$ (interrill erosion) S_p : percentage of land area covered by surface cover R_u : surface roughness
$SR = exp\left\{ -0.66\,(R_u - 0.24) \right\}$	R_u : surface roughness
$SM = 1$	Assumed value in context with limited data

The P factor (Eq. 11) represents the conservation practice in the cropland area and ranges from 0 up to 1, and only depends on the local slope (s_c, in percent). The highest value is assigned to areas with no conservation practices [54]. For the case of Peru, we assumed that contouring practices takes place in moderate ridge heights because the limited collected information, which is not the case in others agricultural practices, such as strip-cropping and terraces that require more detailed data [43].

$$P = \begin{cases} 23.132\,(7 - s_c)^4 + 0.45, & if\ s_c < 7 \\ 12.26\,(s_c - 7)^{1.5} + 0.45, & if\ s_c \geq 7 \\ 1.0, & if\ s_c \geq 20 \end{cases} \tag{11}$$

2.2.3 Data post-processing

Commonly, data post-processing encompasses two main steps, namely: [1] defining the output resolution based on the scale of the region evaluated and the objective of the study [18, 17]; and [2] denoising raw data (mainly C facator) resulting from a downscaling operation. A resolution of 5 km (0.045°), which lays between the lower and upper data sources resolution (see Table 1) is probably the best choice for most of the developing countries. It is important to mention that a finer resolution increases the noise at the raw data mean while a

coarser resolution would result in losing information [56].
For the case of Peru, some C factor pixels, mainly located in the Amazonian region, presented a high bias error and a negligible variance error. These instances represented 0.15% of the whole data and were re-categorized by the k-Nearest Neighbors algorithm appropriately clustering the data (k is the neighborhood size). By following an observational criterion, the parameter k was fixed to a 5-pixel size to ovoid over-clustering the data.

2.3 Model validation

Most of the studies on estimating ERs do not provide a systematic methodology to calibrate the RUSLE model. Herein we propose using the sediment delivery ratio (SDR) as a proxy parameter to calibrate the RUSLE model at a country scale. SDR has been widely applied to validate the ER estimates when basic information is limited [52,43,2]. It represents the ratio between SY and ER, and is mathematically defined by Eq. 12 in which SLP (in %) is the slope of the main stream channel.

$$SDR = 0.627SLP^{0.403} \tag{12}$$

For model validation purposes, it is important to select gauging stations proving SY data that appropriately represents the country's meteorological and topographical spatial variability. Commonly, erosion model results are accepted when the SY rates differ less than 20% from measured SY data [52]. For Peru, SY was quantified for: [1] three watersheds running towards the Pacific Ocean (i.e., Jequetepeque, Chira, and Santa rivers), and [2] the whole Eastern Peruvian Andes. The former estimates were compared with those from the corresponding gauging stations (items M, N and O in Table 1). Likewise, the latter were compared to those obtained by Latrubesse and Restrepo [32], i.e. 1113 $mill\ Ton/year$ of sediments for the Eastern Peruvian Andes.

3 Results and Discussion

As shown in this paper, free satellite data provides valuable information to estimate ERs at country scale. However, the access to such data is currently difficult as they are not easily identifiable through common search portals such as Google. Apparently, globalizing satellite information for the all of potential end users around the world is still pending [22,23,47].
Equations 1 through 11 were used to build eight, four and twelve SE scenarios for the years 1990, 2000 and 2010, respectively (Table 3) and, subsequently, a spatial analysis was performed to obtain ER national maps at 5-km resolution for those years.
The results of the scenarios presented in Table 3 were validated using SY measurements (items M, N and O in Table 1). Figure 2 shows the results in the Jequetepeque, Chira and Santa watersheds as well as those obtained by Latrubesse and Restrepo [32]. In Figure 2, the black line shows the temporal variation of measured SY rates; likewise, the gray shadow strip represents the acceptable area limited by upper and lower 20% deviation margins.
Our results revealed that the SY rates in the Santa (10415 km^2), Chira (6343 km^2), and Jequetepeque rivers (3317 km^2) are proportional to the basin area. Past studies show that SY both increase and decrease as a function of drainage area [17]. Likewise, the highest SY rate corresponds to the year 1998 which is related to a severe El Niño event that occur in such year.

Table 3 Scenarios evaluated for the years 1990, 2000 and 2010

Scenarios	R factor Source	Equation	C and P factors Source
Year: 1990			
Scenario 1.1	GPCP	Arnoldus	USGS EROS Data Center
Scenario 1.2	GPCP	Arnoldus	ONERM
Scenario 2.1	GPCP	Renard and Freimund	USGS EROS Data Center
Scenario 2.2	GPCP	Renard and Freimund	ONERM
Scenario 3.1	Ground Stations	Arnoldus	USGS EROS Data Center
Scenario 3.2	Ground Stations	Arnoldus	ONERM
Scenario 4.1	Ground Stations	Renard and Freimund	USGS EROS Data Center
Scenario 4.2	Ground Stations	Renard and Freimund	ONERM
Year: 2000			
Scenario 1	GPCP	Arnoldus	MODIS Land Cover
Scenario 2	GPCP	Renard and Freimund	MODIS Land Cover
Scenario 3	Ground Stations	Arnoldus	MODIS Land Cover
Scenario 4	Ground Stations	Renard and Freimund	MODIS Land Cover
Year: 2010			
Scenario 1.1	TRMM	Arnoldus	MINAM
Scenario 1.2	TRMM	Arnoldus	FAO
Scenario 1.3	TRMM	Arnoldus	MODIS Land Cover
Scenario 2.1	TRMM	Renard and Freimund	MINAM
Scenario 2.2	TRMM	Renard and Freimund	FAO
Scenario 2.3	TRMM	Renard and Freimund	MODIS Land Cover
Scenario 3.1	Ground Stations	Arnoldus	MINAM
Scenario 3.2	Ground Stations	Arnoldus	FAO
Scenario 3.3	Ground Stations	Arnoldus	MODIS Land Cover
Scenario 4.1	Ground Stations	Renard and Freimund	MINAM
Scenario 4.2	Ground Stations	Renard and Freimund	FAO
Scenario 4.3	Ground Stations	Renard and Freimund	MODIS Land Cover

Note: K, L and S are static factors.

In most of the instances, the scenarios in which the R factor was obtained from meteorological ground measurements (gray point markers in Fig. 2), SY estimates lay outside of the acceptable area. On the other hand, the scenarios in which the R_{RF} factor is used as input parameter (blue, black and red points markers in Fig. 2), SY estimates lay inside the acceptable area.

As expected, the accuracy of the results from the aforementioned scenarios exhibit both temporal and spatial variability. For example, for the year 1990, scenario 2.1 (black points in Figs. 2.a and 2.b) results on $SY = 0.34\ mill\ m^3/year$ in Jequetepeque basin which lays inside the acceptable area, and $SY = 0.57\ mill\ m^3/year$ in Chira basin which lays outside the acceptable area. Similarly, for the year 2000, scenario 2 (blue points in Figs. 2.a-b), SY rates of 3.53 and 6.36 mill m^3/year were obtained in the Jequetepeque and Chira basins respectively, which lay close to acceptable area. Likewise, in the Amazonian region (Fig. 2.d), the SY estimate from scenario 2 is located inside the acceptable area; in contrast, in the Santa basin (Fig. 2.c) the SY rate is lower than the acceptable range. For the year 2010, SY estimates from scenarios 2.1 (red points) and 2.2 (black points) are acceptable in the Pacific basins; however, results from scenario 2.1 (red points) lay outside the acceptance area in the Amazonian region (Fig. 2.d). Most of the SY estimates in Chira basin (Fig. 2.b) lay outside

the acceptable area, this performance is possibly triggered by El Niño Southern Oscillation which plays an important role in the erosion processes in the Peruvian northern coast [26]. In conclusion, the scenario 2.1 is acceptable for the year 1990, scenario 2 for the year 2000, and scenario 2.2 for the year 2010. Figure 3 and Online Resource 1 (in kmz format) present the country ER maps obtained from such scenarios.

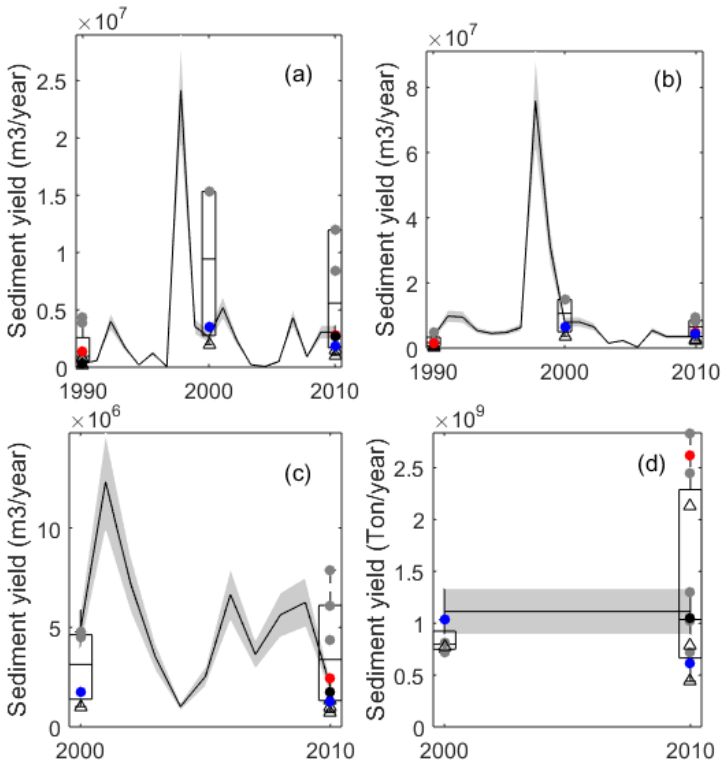

Fig. 2 Validation of the RUSLE model scenarios for the years 1990, 2000 and 2010 for: (a) Jequetepeque, (b) Chira, (c) Santa, and (d) Eastern Peruvian Andes. The black line represents SY data from gauging stations and the gray strip, the acceptable area which is bounded by the upper and lower 20% deviation from the black line. Gray points shows the scenarios 3.1 to 4.2 for the year 1990, scenarios 3 to 4 for the year 2000, and scenarios 3.1 to 4.3 for the year 2010. Triangle markers represent scenarios 1.1 and 1.2 for 1990, scenario 1 for the year 2000 and scenarios 1.1 to 1.3 for the year 2010. Black points represent the scenario 2.1 in 1990 and 2.2 in 2010. Red points represent scenarios 2.2 in 1990 and 2.1 in 2010. The blue points present the scenarios 2 in 2000 and 2.3 in 2010.

The 1990 map (Fig. 3.a) shows that in most of the territory, especially in the Amazonian region, ER was $< 10\,ton/ha/year$. This result has a similar order of magnitude to that from the climatic erosion potential index published in 1993 [16] which presents a scale of erosion of $10\,ton/ha$ for the whole Amazonian region. Our results for Andean ($20-100\,ton/ha/year$) and the Amazonian regions ($10\,ton/ha/year$) are also comparable to those of the global yearly averaged ER map of [18].

The 1990, 2000 and 2010 ER maps we obtained (Fig. 3.a-c) show that the highest ER estimates ($> 50\,ton/ha/year$) are located in the Andean region. These results are explained

by the fact that this region presents steep slopes and periods of high rainfall which have an essential role in the production of SY and SE [1]. High ERs are also observed in the coastal area which are the result of an increase in the C factor, i.e. land use change, induced by an steadily growing of farming and urban areas, and population (e.g., from 2007 to 2014, the Peruvian population that lived in the coastal area grew from 54.6% through 63.4%) [57–60]. Likewise, the coastal region is characterized as a high activity seismic region in which endogenic processes (i.e. earthquakes) and exogenic processes (i.e., soil erosion and landslides) are positively correlated [61,62]. Conversely, low ERs are observed in the Amazonian region where the dense vegetative land cover inhibits SE to progress.

A temporal and spatial analysis of ER from reveals that moderate ERs ($10-50\,ton/ha/year$) have notably increased in the the western Peruvian Andes and along the coast region for the periods 1990-2000 (Fig. 3.d) and 2000-2010 (Fig. 3.e). These changes are mainly triggered by changes in land use [63].

For the year 2010, Moquegua and Apurimac provinces (which are located in the southern Peruvian region, as shown in Fig. 3.f) have been severely affected by erosion in the 60% of their area approximately (Fig. 4). This scenario can potentially get worse if the illegal mining practices and SE are not properly controlled.

The national erosion rate shows an steady increase for the years 1990 ($19\times10^6\ ton/year$), 2000 ($26\times10^6\ ton/year$), and 2010 ($41\times10^6\ ton/year$) and it is expected to keep such trend because changes in land use are expected due to the increase of areas granted to the extractive industry [29]. Mining, for example, commonly triggers dry-land hill-slopes areas which are highly sensitive to generate significant amounts of SY even during relatively low rainfall intensities [1]. Under the light of these results, we believe that a erosion control regulatory framework is possibly needed in Peru.

In recent years, some scientific and intergovernmental groups have highlighted the need to advance broad open data policies and practices, and foster the increased use of Earth observation data [47]. We believe that the method we elaborate herein not only contributes to these ends but also has the potential to become an initial standard frame to quantify ERs in developing countries, and subsequently guide the decisions ans actions to manage their soil resources.

4 Conclusions

This study elaborates on a RUSLE-based method to obtain national erosion rate maps for developing countries. It combines up-to-date global publicly available data from satellite measurements, global soil and land cover models, and conventional ground-based data. Thus, it is pursued globalizing the societal benefits of satellite remote sensing data which potentially overcomes those of conventional ground-based measurements in developing countries. The method proposes the use of the sediment delivery ratio as a proxy parameter to validate the RUSLE model, and is successfully applied to obtain ER country maps for Peru. The results show that Peru faces an steady increase of ERs 1990 ($19\times10^6\ ton/year$ for 1990, $26\times10^6\ ton/year$ for 2000, and $41\times10^6\ ton/year$ for 2010) and, apparently, it will keep such trend because its economy relies mainly on extractive industries, it is expanding its infrastructure portfolio, and its urban population is growing. Probably such is also the case of many developing countries. Thus, this proposed method has the potential to guide decision makers towards a better soil resources management in such countries.

Although our results are in the same order of magnitude as previous global scale erosion rates maps, future studies to quantify country R, K, and C factors are needed. Some devel-

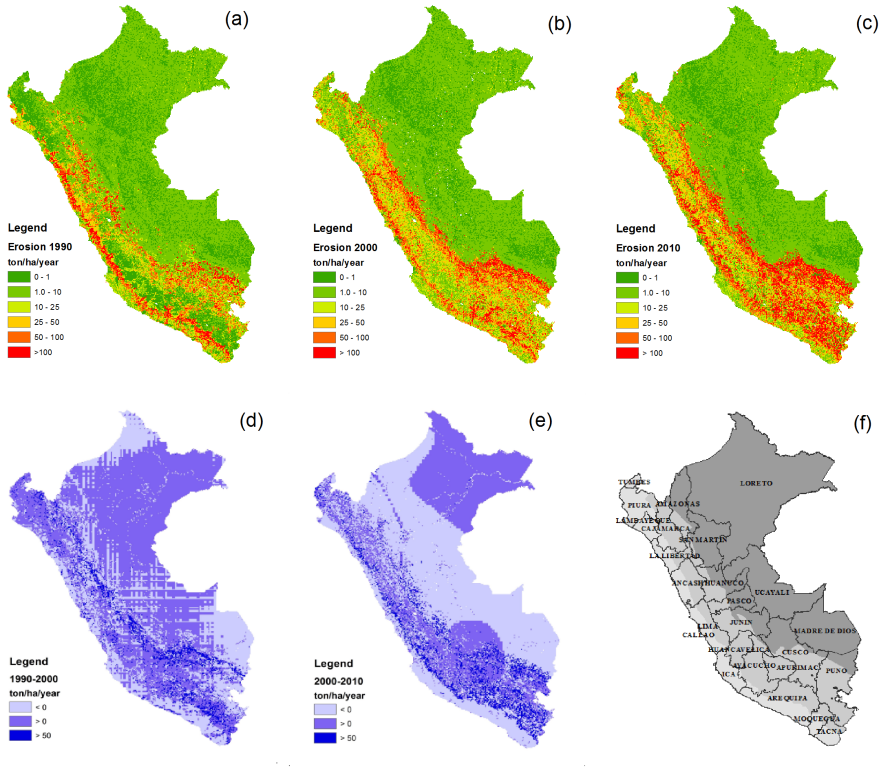

Fig. 3 RUSLE model output for Peru at 5-km resolution. Maps (a), (b) and (c) show erosion rates for the years 1990, 2000 and 2010, respectively. Map (d) presents the ER gradient between the years 1990 and 2000, and map (e), those for the years 2000 and 2010. Figure (f) shows the Peruvian political map (gray shadows represent the Coastal, Andean, and Amazonian regions).

oping countries are already going in such direction.
In the light of our results, we believe that an erosion control regulatory framework should be seriously considered for Peru.

Supporting Information

Interactive Peruvian soil erosion maps for the years 1990, 2000 and 2010 in .kmz format.

Acknowledgements Authors thank the financial support provided by the Consejo Nacional de Ciencia y Tecnologia, and the valuable data provided by the Servicio Nacional de Meteorologia e Hidrologia and the Instituto Geofisico del Peru. The authors also appreciate the technical discussions with Dr. Waldo Lavado and Dr. Sergio Morera.

References

1. K. Michaelides, G.J. Martin, Journal of Geophysical Research **117** (2012)

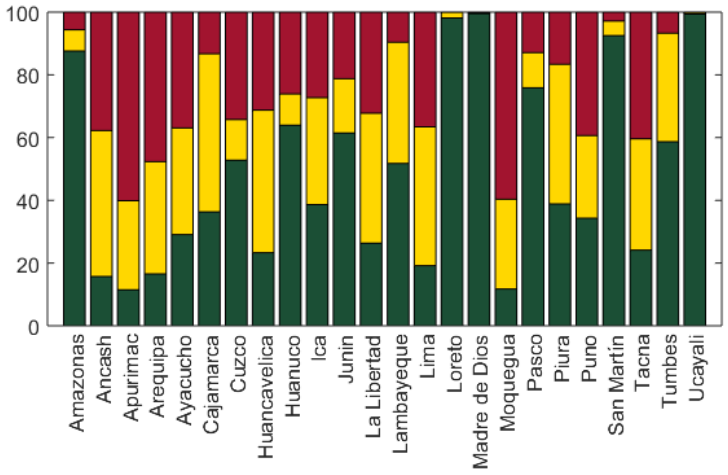

Fig. 4 Categorical distribution of soil erosion in Peruvian provinces for the year 2010. Green, yellow and red bars represent slight ($< 10\ ton/ha/year$), moderate ($10 - 50\ ton/ha/year$), and severe erosion rates ($> 50\ ton/ha/year$), respectively.

2. J. Onyando, P. Kisoyan, M. Chemelil, Water Resources Management **19**, 133 (2005)
3. Pierre Y. Julien, *Erosion and sedimentation* (Cambridge University Press, New York, USA, 2010)
4. R. Evans, Applied Geography (22), 187 (2002)
5. M.O. Ribaudo, in *The Management of Water Quality and Irrigation Technologies*, ed. by J. Albiac, A. Dinar (Earthscan, 2009)
6. G.K. AAyele, A.A. Gessess, M.B. Addisie, S.A. Tilahum, T.Y. Tebebu, D.B. Tenessa, C.F. Langendoen, Eddy J. nad Nicholson, T.S. Steenhuis, Land Degradation and Development pp. n/a–n/a (2015)
7. A. Van Rompaey, G. Verstraeten, K. Van Oost, G. Govers, J. Poesen, Earth Surface Processes and Landforms **26**(11), 12211236 (2001). URL doi: 10.1002/esp.275
8. R. Young, C. Onstad, D. Bosch, W. Anderson, Journal of Soil and Water Conservation **44**(2), 168 (1989)
9. A. de Roo, C. Wesseling, C. Ritsema, Hydrological Processes **10**(8), 1107 (1996)
10. J. de Vente, J. Poesen, G. Verstraeten, G. Govers, M. Vanmaercke, A. Van Rompaey, M. Arabkhedri, C. Boix-Fayos, Earth-Science Reviews (127), 16 (2013)
11. K.G. Renard, J.R. Freimund, Journal of Hydrology **157**, 287 (1994)
12. W. Merritt, R. Letcher, A. Jakeman, Environmental Modelling and Software **18**(89), 761 (2003)
13. J. Boardman, J. Poesen, (John Wiley and Sons, 2006)
14. R. Morgan, M. Nearing, *Handbook of Erosion Modelling* (Wiley-Blackwell, UK, 2011)
15. N. Bellin, V. Vanacker, B. van Wesemael, A. Solé-Benet, M. Bakker, Catena **87**(2), 190 (2011)
16. M. Kirkby, N. Cox, CATENA **1-4**, 333 (1995)
17. A. Cerdà, R. Brazier, M. Nearing, J. de Vente, CATENA **102** (2013)
18. V. Naipal, C. Reick, J. Pongratz, K. Van Oost, Geoscientific Model Development **8**, 2893 (2015)
19. M. Masoudi, *Risk Assessment and Remedial Measure of Land Degradation, in parts of Southern Iran* (LAP LAMBERT Academic Publishing, Saarbücken, USA, 2010)
20. A. Shamshad, C. Leow, A. Ramlah, W. Wan Hussin, S. Mohd. Sanusi, International Journal of Applied Earth Observation and Geoinformation **10**(3), 239 (2008)
21. E.F. Wood, J.K. Roundy, T.J. Troy, L.P.H. van Beek, M.F.P. Bierkens, E. Blyth, A. de Roo, P. Dll, M. Ek, J. Famiglietti, D. Gochis, N. van de Giesen, P. Houser, P.R. Jaff, S. Kollet, B. Lehner, D.P. Lettenmaier, C. Peters-Lidard, M. Sivapalan, J. Sheffield, A. Wade, P. Whitehead,
22. F. Hossain, Bullletin of the American Meteorological Society **93**, 1633 (2012)
23. Hossain F., EOS Earth Planet and Space **96** (2015)
24. S.B. Morera, T. Condom, P. Vauchel, J.L. Guyot, C. Galvez, , A. Crave, Hydrology and Earth System Sciences **17**(11), 4641 (2013). DOI 10.5194/hess-17-4641-2013. URL http://www.hydrol-earth-syst-sci.net/17/4641/2013/
25. R. Espinoza, J.M. Martinez, M. Le Texier, J.L. Guyot, P. Fraizy, P.R. Meneses, E. de Oliveira, Journal of South American Earth Sciences **1**(10) (2012)

26. W.H. Quinn, V.T. Neal, S.E. Antunez De Mayolo, Journal of Geophysical Research **92**(C13), 1444914461 (1987). URL 10.1029/JC092iC13p14449
27. K. Takahashi, A. Montecinos, K. Goubanova, B. Dewitte, Geophysical Research Letters **38**(10) (2011). L10704
28. A.J. Vuohelainen, L. Coad, T.R. Marthews, Y. Malhi, T.J. Killeen, Environmental Management **50**(4), 645 (2012). DOI 10.1007/s00267-012-9901-y
29. OXFAM, Geographies of conflict: Mapping overlaps between extractive industries and agricultural land uses in Ghana and Peru. Tech. rep., OXFAM America, USA (2014)
30. M. Vuille, B. Francou, P. Wagnon, I. Juen, G. Kaser, B.G. Mark, R.S. Bradley, Earth-Science Reviews **89**, 70 (2008)
31. Instituto Nacional de Recursos Naturales, *Memoria Descriptiva: Mapa de Erosión de los Suelos del Perú.* (Ministerio de Agricultura, Lima, Perú, 1996)
32. E.M. Latrubesse, J.D. Restrepo, Geomorphology **216**, 225 (2014)
33. R. Adler, G. Huffman, A. Chang, R. Ferraro, P. Xie, J. Janowiak, B. Rudolf, U. Schneider, S. Curtis, D. Bolvin, A. Gruber, J. Susskind, P. Arkin, Journal of Hydrometeorology **4**, 1147 (2003)
34. G. Huffman, R. Adler, D. Bolvin, G. Gu, E. Nelkin, K. Bowman, Y. Hong, E. Stocker, D. Wolff, Journal of Hydrometeorology **8**(1), 38 (2007)
35. ISRIC World Soil Information. SoilGrids: an automated system for global soil mapping. Available for download at http://soilgrids1km.isric.org. (2013)
36. METI and NASA. ASTER Global Digital Elevation Model (ASTER GDEM) . Available for download at http://gdem.ersdac.jspacesystems.or.jp/ (2011)
37. ORNL DAAC. 8 km Global Land Cover Data Set Derived from AVHRR. Available for download at http://webmap.ornl.gov/wcsdown/index.jsp (2011)
38. T. Loveland, B. Reed, J. Brown, D. Ohlen, J. Zhu, L. Yang, J. Merchant, International Journal of Remote Sensing **21**(6/7), 303 (2000)
39. S. Channan, K. Collins, W.R. Emanuel, *Global mosaics of the standard MODIS land cover type data* (University of Maryland and the Pacific Northwest National Laboratory, College Park, Maryland, USA, 2011)
40. J. Latham, R. Cumani, I. Rosati, M. Bloise, *Global Land Cover SHARE database Beta-Release Version 1.0* (Food and Agriculture Organization of the United Nations,FAO, Rome, Italy, 2014)
41. R.F. Adler, G.J. Huffman, A. Chang, R. Ferraro, P.P. Xie, J. Janowiak, B. Rudolf, U. Schneider, S. Curtis, D. Bolvin, A. Gruber, J. Susskind, P. Arkin, E. Nelkin, Journal of Hydrometeorology **4**, 1147 (2003)
42. G.L. Stephens, T. L'Ecuyer, R. Forbes, A. Gettlemen, J.C. Golaz, A. Bodas-Salcedo, K. Suzuki, P. Gabriel, J. Haynes, Journal of Geophysical Research: Atmospheres **115** (2010). D24
43. V. Jetten, M. Maneta, in *Handbook of erosion modelling*, ed. by M. R.P.C., N. M.A. (Wiley Blackwell Publishing, 2011)
44. G.E. Frey, H.E. Fassolab, A.N. Pachas, S.M. Colcombetb, Luis an Lacortec, O. Prezd, M. Renkowe, S.T. Warrenf, F.W. Cubbage, Agricultural Systems **105**(1), 21 (2012)
45. L. Brandimarte, A. Brath, A. Castellarin, G. Di Baldassarre, Physics and Chemistry of the Earth **34**, 209 (2009)
46. G. Kasera, I. Juen, C. Georgesa, J. Gomez, W. Tamayo, Journal of Hydrology **282**, 130 (2003)
47. R. Showstack, EOS **96** (2015)
48. C. Bonilla, K.L. Vidal, Journal of Hydrology **410**, 126 (2011)
49. S.H. Franchito, A.C. Vasquez, J. Coronado, Journal of Geophysical Research: Atmospheres **114**(D2) (2009)
50. Z.D. Adeyewa, K. Nakamura, J. Appl. Met. **42**(2), 331 (2003)
51. Fonseca, Sigfredo E. and Reategui, Pamela, *Elaboracion de mapas de isoyetas - Ambito politico administrativo y unidades hidrograficas.* (Autoridad Nacional del Agua, ANA, Lima, Perú, 2012)
52. L. Hui, C. Xiaoling, K.J. Lim, C. Xiaobin, M. Sagong, Journal of Earth Science **21**(6), 941 (2010)
53. S.E. Nicholson, *Dryland Climatology* (Cambridge University Press, United Kingdom, 2011)
54. K. Renard, G. Foster, G. Weesies, D. McCool, D. Yoder, *Predicting Soil Erosion by Water: A Guide to Conservation Planning with the Revised Universal Soil Loss Equation*. United States Department of Agriculture (1997)
55. Soil Survey Staff, *Kellogg Soil Survey Laboratory Methods Manual. Soil Survey Investigations Report No. 42, Version 5.0.* U.S. Department of Agriculture, Natural Resources Conservation Service (2014)
56. L. Martin-Fernandez, M. Martinez-Nuñez, Sciences of the Total Environment **409**, 3114 (2011)
57. M. Paulet Iturri, C. Amay Leon, *La conservacion de seulos en la sierra de Peru. Sistematizacion de la experiencia de Pronamachs en la lucha contra la desertificacion* (IIICA Consorcio tecnico, Lima, Peru, 1999)
58. World Development Indicators: Agricultural inputs. Tech. rep., The World Bank Group, USA (2015)

59. Direccion general de seguimiento y evaluacion de politicas, *Informe de Seguimiento Agroeconomico I Trimestre 2015* (Ministerio de Agricultura y Riego, Lima, Peru, 2015)
60. Instituto Nacional de Estadistica e Informatica, *Peru: Poblacion estimada al 30 de junio y tasa de crecimiento de las ciudades capitales, por departamento, 2014* (INEI, Peru, 2014)
61. A. Scheidegger, Geomorphology **5**, 213 (1992)
62. A. Scheidegger, N. Ai, Tectonophysics **126**(2-4), 285 (1986)
63. N. Ramankutty, A. Evan, C. Monfreda, J. Foley, Global Biogeochemical Cycles **22**, 1 (2008)

CAPITULO 3:

Sediment yield changes in the Peruvian Andes for the year 2030

Sediment yield changes in the Peruvian Andes for the year 2030

Miluska A. Rosas[1], Ronald R. Gutierrez[2]

[1]*Graduate Student, School of Civil Engineering, Pontifical Catholic University of Peru*
[2]*Associate Professor, School of Civil Engineering, Pontifical Catholic University of Peru*

Abstract

The amount of sediment yield produce in the Peruvian Andes have a high significance specially in the Amazon basin, however few studies have addressed to quantify the volume of sediments in a country and continental scale for the next years. To estimate the sediment yield for the year 2030, a land cover change model has been build, which is based on 1990, 2000 and 2010 land cover/land use maps. This model predict three scenarios: the normal scenario, the scenario in which the mining activity is included, and the scenario that presents protected areas. Our results predict that the volume of sediments produced in the Amazon basin ($2115 Ton/year$) will be higher than in the Pacific basin ($932 ton/year$) for the year 2030, also the scenario that includes the mining activities induce an increase of sediments in both basins, conversely, the scenario that includes the protected areas inhibit the soil erosion process.

Keywords: soil erosion, sediment yield, land cover change, Amazon basin

1. Introduction

Sediment yield (SY) is the result of erosion and deposition processes within a basin, which is basically controlled by local topography, soil and weather properties, land cover and land use, catchment morphology, drainage network characteristics, among others [1], which commonly induces the lost of fertile topsoil for agriculture and the siltation of streams and lakes [2].
The Amazon river carries a significant amount of suspended sediment load from the South America continent [1]. Limited number of studies have quantified SY in the upper Amazon (tropical rivers), which comprises the territories of Peru and Bolivia.Latrubesse and Restrepo [3] estimated that this region approximately produces 60% of the SY in the whole Andes, in addition Rosas and Gutierrez [4] obtained Peruvian erosion rate (ER) maps for the year 1990, 2000 and 2010, these results provide valuable information to indirectly quantify the SY in such region.
Peru is affected by the El Niño/La Niña Southern Oscillation which is the main source of temperature and climate variability [4, 5], in addition, Peru is a developing country and significant change in land use cover is expected in the medium term [6]. However, few studies exist about future predictions induced by global warming, land use change and urban growth in the country. Some researchers have highlighted the fact that the dataset is not representative and insufficient to obtain reliable future estimates in developing countries, in the light of this context, [7] mentions that the satellite data have the capability to face this gap in time and spatial terms.
Land cover/land use distribution is the most sensitive variable to estimate ER [4], land cover change models are used in many studies of human impacts on the environment, e.g. deforestation practices, some of this models are based on logistic regression, multi-layer perceptron neural

network and K-nearest neighbor machine learning algorithm, among others [8].
The purpose of this this paper is quantifying the SY in the Pacific basin and Amazon region in the Peruvian territory for the year 2030, the impacts of three scenarios have been analyzed, namely: normal, including mining practices and including protected areas. Firstly, land cover change scenarios for Peru have been built in the IDRISI platform for the year 2030, subsequently, with the purpose to indirectly quantify the SY in the Pacific basin and Amazon region, the Revised Universal Soil Loss Equation (RUSLE) and the sediment delivery ratio (SDR) methodologies have been applied. RUSLE is widely used to predict SE around the world [9] and SY is usually obtained from erosion rate (ER) estimates by applying the SDR methodology in limited data contexts [10].

2. Materials and Methods

2.1. Land cover change model

2.1.1. Data source

To the best of our knowledge, information about the land cover change in Peru for the next decades does not exists, the last official land use map was published in 2010 and it classify the area in 39 types of lands.
The data used herein comprises the main drivers driver of land change, which commonly occurs near to vial infrastructure, cities and human economic activities (e.g. mining practices in the case of Peru). Geographical, topographical, and land cover information were collected to represent these drivers (Table 1), such data was obtain from Peruvian public agencies and free available satellite international sources.

Table 1: Input data used

Item	Name	Source	Resolution	Year
A	Digital Elevation Model	Japan Space System	30 m	2009 - 2011
B	Principal cities (shapefile)	Ministerio Nacional de Educacion, MED	-	2011
C	Major roads (shapefile)	Ministerio Nacional de Transporte y Comunicaciones, MTC	-	2011
D	Actual and projected mining areas (shapefile)	Ministerio de Energia y Minas	-	2011
E	Protected areas (shapefile)	Ministerio Nacional del Ambiente, MINAM	-	2011
F	Global Land Use/Land Cover images (15 classes)	USGS EROS Data Center	0.1°	1992-93
G	The Global Land Cover Facility (16 classes)	MODIS Land Cover	0.25′	2001
H	Global Land Cover Share Database (10 classes)	FAO, Land and Water Division	1km	2014

In order to compare the changes between the land cover maps for the year 1990, 2000 and 2010 (items F, G and H in Table 1, the data was reclassified to harmonize the land cover number and classes. Eight land cover classes have been defined: urban and built, wooded wetland, snow and ice, tree covered (TC), woody savannas (WS), grassland and shrubs (GS), cropland (CR) and barren or sparsely (BS), table 2 shows a description of each land cover class.

2.1.2. Model structure

A prediction model structure has been build in IDRISI Selva software with the tools of the Land Change Modeler (LCM) platform. LCM in an empirically process that involves: change analysis, transition potential modeling and change prediction, which is based on the historical change between two time-periods with the purpose of building future scenarios [8].
Firstly, the land cover changes between the years 1990 and 2000 has been analyzed, the LCM

Table 2: Description of the land covers selected

Land cover classes	Description
Urban and built	Lands covered by buildings and other infrastructure.
Wooded wetland	Lands with a permanent mixture of water and herbaceous or woody vegetation that cover extensive areas. The vegetation can be present in either salt, brackish, or fresh water.
Snow and ice	Lands under snow and/or ice cover throughout the year.
Tree covered (TC)	Land dominated by trees with a percent canopy cover of greater than 60% and height exceeding 2 meters.
Woody savannas (WS)	lands with herbaceous and other understory systems, and with forest canopy cover between 3060%. The forest cover height exceeds 2 meters.
Grassland and shrubs (GS)	Lands with herbaceous types of cover. Tree and shrub cover is less than 10%.
Cropland (CR)	Lands covered with temporary crops followed by harvest and a bare soil period.
Barren or sparsely (BS)	Lands of exposed soil, sand, rocks, or snow and never has more than 10% vegetated cover during any time of the year.

platform has identified two important transitions: from TC to GS and from WS to GS, however, due to the mining activity increase in the country, three additional transitions have been considered, from TC to BS, from GS to BS and from CR to BS.

To built the transition sub-models, the variables have been selected by a tested based on the Cramer factor, which is a measure of inter-correlation of two variables and it is based on goodness of fit Pearson's chi-squared statistic models [11]. Cramer values lower than 0.15 are unacceptable and values upper 0.4 has a high level of significance [8] (see Fig. 1). The variables have been gathered in two categories: static and dynamic, the former are calculated ones in the beginning of the modeling process, and the later are re-calculated in each time step (two years) [12]. Static variables are composed by elevation and slope (from item A in table 1), and dynamic variables are composed by distances to cities (from item B in table 1), distance to roads (from item C in table 1), and distance to the actual mining areas (from item B in table 1). Additionally, the variable likehood to BS has been added with LCM platform with the purpose of modeling the impact of the mining activity. Each transition has been modeled using the multi-layer perception neural network which has the capability to evaluate multiple transitions in one model using Markov chains [8, 13].

2.1.3. Model Validation

The performance of the model prediction for the year 2010, has been evaluated by the receiver operating characteristic (ROC) curve, which is commonly applied in land cover change studies to measures the agreement of the predicted and the observed values of change, in terms of the true positives (correct change) against the false positives (errors) in the predicted model, models whit ROC value upper 0.5 have a high significance [14, 15, 16]. Additionally, a pixel-by-pixel comparison, has been calculated, between the observed (item H in table 1 Figure 2.a) and predicted land cover map for the year 2010. Such comparison is composed by three measures of precision, namely: hits (model predicted change and it change), false alarm (model predict change and it persisted), and misses (model predicted persistence and it changed), it provide more information and a spatial distribution of errors [17].

2.2. Model scenarios 2030

For the year 2030, three predictive model scenarios have been tested, namely: normal scenario, mining activity scenario (scenario A) and protected areas scenario (scenario B). Normal scenario

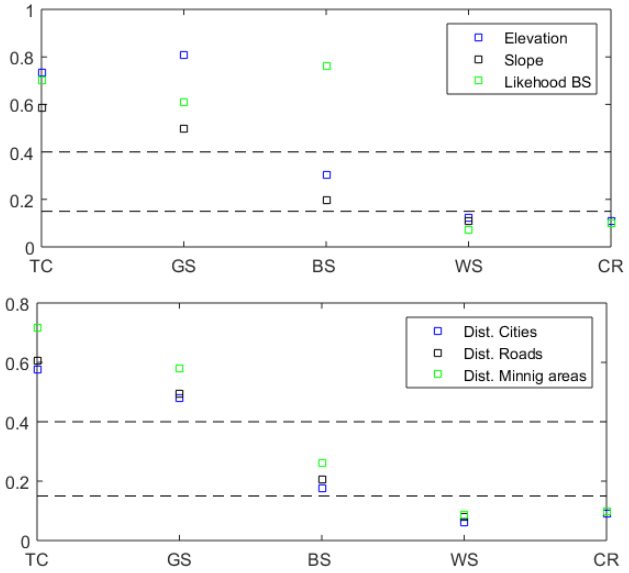

Figure 1: Cramer values for static (figure above) and dynamic (figure below) variables.

presents the application of the variables and the transition sub-models mentioned in section 2.1.2 estimated from the 1990 and 2000 land cover maps, it represents the land change baseline in the country, scenario A includes the predicted areas granted to mining concession (item D in table 1) which are more sensibles to hydraulic erosion process. Finally, scenario B, includes protected areas (item E in table 1) that simulates the less SE impact in such areas.

2.3. Soil erosion and sediment yield

Revised Universal Soil Loss Equation (RUSLE) model have been widely applied in a large scales, although it presents various limitations [18]. RUSLE is mathematically defined by Eq. 1.

$$A = R \times K \times L \times S \times C \times P \tag{1}$$

where A is annual soil erosion ($t\ ha^{-1}\ year^{-1}$); R is the rainfall erosivity factor ($MJ\ mm\ ha^{-1}\ h^{-1}\ year^{-1}$); K is the soil erodibility factor ($t\ h\ MJ^{-1}\ mm^{-1}$); L is the slope length factor; S is the slope steepness factor; C is the cover management factor; and P is the conservation supporting practices factor (L, S, C and P are dimensionless). These variables were separated into static and dynamic sets. The former represents features that stay constant in time such as K, L and S; conversely, R, C and P were classified as dynamic, because they are time sensitive.

Sediment delivery ratio (SDR) is widely applied to stimate SY in context with limited information (i.e., [10, 19, 20]). SDR is the rate between the SY and the ER and is defined by Eq. 2, in which SLP (%) is slope of the main stream channel based on the stream length and the altitude difference [10]. Thus, the indirect SY estimation was based on the ER and SDR ratio.

$$SDR = 0.627 SLP^{0.403} \tag{2}$$

The main databases to obtain SE and SY for the year 2030 are the land cover change predicted (see section 2.1) and the Peruvian precipitation 2030 map provided by Servicio nacional de meteorologia y recursos hidricos (Senamhi). For details on the data bases and quantification ER and SY, the reader is kindly referred to Rosas and Gutierrez [4].

3. Results and Discussion

The land cover change model has been built with five recalculation stages (time step: two years) in the LCM platform to obtain the predicted land cover map for the year 2010 (Fig. 2b). This model presents high ROC values: 0.63 in the coastal area, 0.72 in highland and 0.94 in the rain-forest. Additionally, the model predicted (Fig. 2.b) and observed data (Fig. 2.a) have been compared pixel by pixel and the model predicted show just 4% of hits (Fig. 2.c). These results suggest that the model has the ability of predict the general spatial patterns ($ROC > 0.5$), but it is not the case for the exact temporal sequence prediction of the change, this is described as one of the difficulties in land cover change models [21].

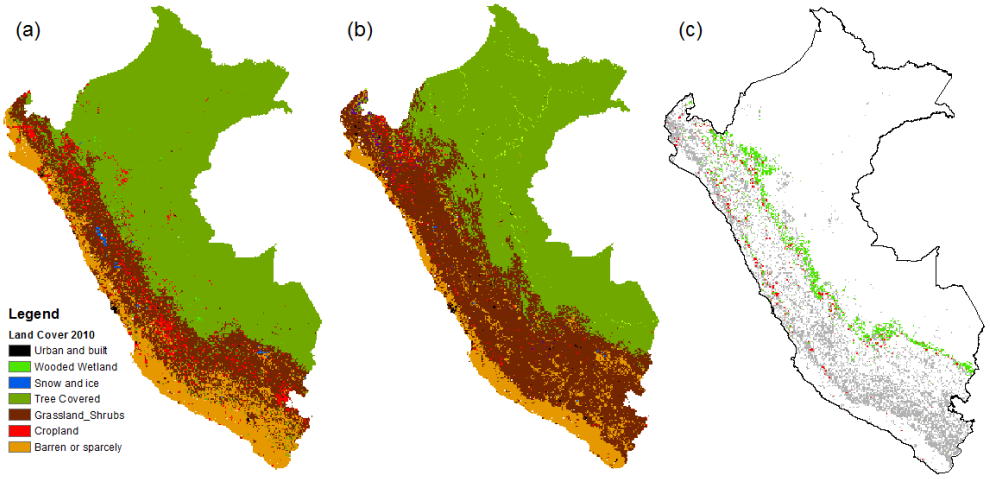

Figure 2: Observed (a) and predicted (b) Peruvian land cover map for the year 2010. The pixel by pixel validation map (c) shows the hits in red, the false alarm in green and the misses in gray

This model has been applied to obtain the three land cover model scenarios (Fig. 3), and subsequently the SE maps for the year 2030 (Fig. 4) by applying the RUSLE equation (for details see section 2.3). Figure 4.b show a notably increase of severe SE rate ($> 100 ton/ha/year$) in the highland region, conversely, in the case of SE controlled by protecting some natural areas (Fig. 4.c) the rates decrease.

Applaying the SDR relationship, SY rates have been obtained for the Peruvian Pacific basin and the Amazon basin for the three predicted scenarios, figure 5 shows that the amount of SY in the Amazon basin is higher than Pacific basin all the scenarios.

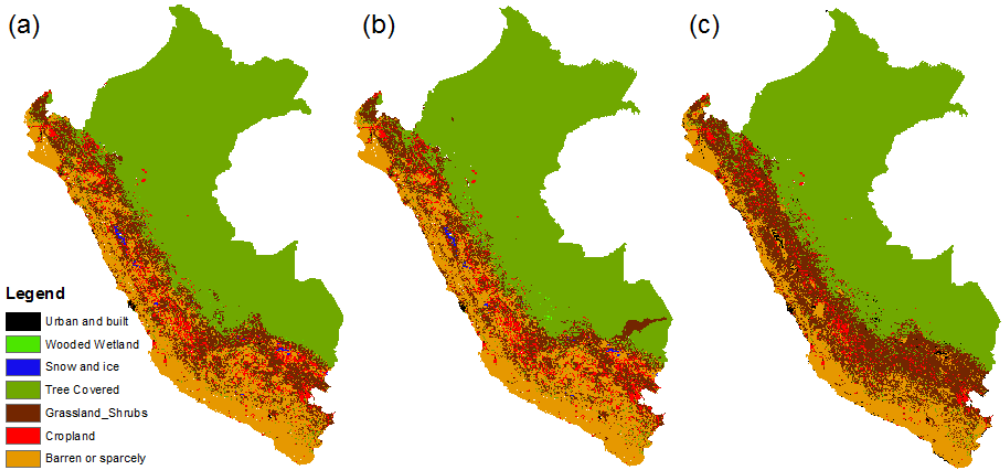

Figure 3: Predicted land cover maps for the year 2030. Normal scenario (a), scenario A (b), which includes mining activities and scenario B (c), which includes protected areas.

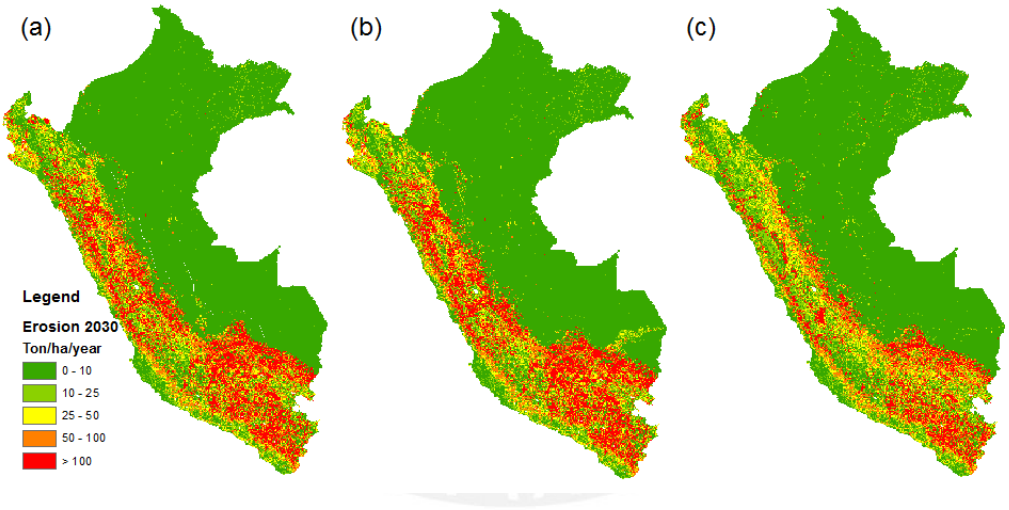

Figure 4: Soil erosion for the year 2030. Normal scenario (a), scenario A (b), which includes mining activities and scenario B (c), which includes protected areas.

4. Conclusion

This study presents a methodology to indirectly quantify SY along the Peruvian Andes, based on land cover change predictions with the purpose to fill the gap of data from ground stations and provide valuable information for decision makers in terms of SE and SY regulation.
Our study clearly reflects that need to obtain prediction maps for the future years, e.g. 2050, which should include global warming aspects and the increase of economic activities in Peruvian context.

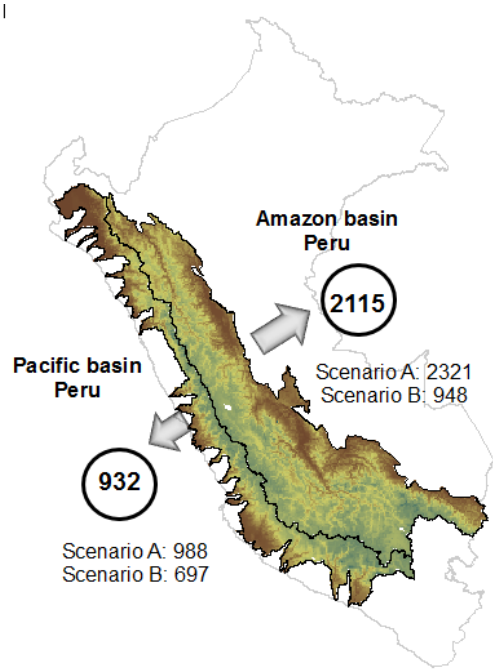

Figure 5: SY rates for the Peruvian Amazon and Pacific basin ($x10^6 Ton/year$). The figure presents the rate for the normal scenario (circles), scenario A (including areas granted to mining activities) and scenario B (including protected areas)

Acknowledgement

Authors are gratefully acknowledged the financial support provided by the by Concytec which is the Spanish acronym for the National Science Foundation in Peru.

References

[1] J. D. Restrepo, B. Kjerfve, M. Hermelin, J. C. Restrepo, Factors controlling sediment yield in a major South American drainage basin: the Magdalena River, Colombia, Journal of Hydrology 316 (2006) 213–232.

[2] M. R. Rahman, Z. Shi, C. Chongfa, Soil erosion hazard evaluationAn integrated use of remote sensing, GIS and statistical approaches with biophysical parameters towards management strategies, Ecological Modelling (2009) 1724–1734.

[3] E. M. Latrubesse, J. D. Restrepo, Sediment yield along the Andes: continental budget, regional variations, an comparisons with other basins from orogenic mountain belts, Geomorphology 216 (2014) 225–233.

[4] M. A. Rosas, R. R. Gutierrez, On a methodology to estimate hydraulic erosion rates in developing countries, Science of the Total Environment (2015).

[5] J. M. Wallace, E. M. Rasmusson, T. Mitchell, E. S. Kousky, V. E.and Sarachik, H. von Storch, On the structure and evolution of enso-related climate variability in the tropical pacific: Lessons from toga, Journal of Geophysical Research 103 (1998) 14,241–14.259.

[6] A. van Soesbergen, M. Mulligan, Modelling multiple threats to water security in the Peruvian Amazon using the WaterWorld policy support system, Earth System Dynamics Discussions 4 (2013) 567–594.

[7] Hossain F., Data for all: Using satellite observations for social good, EOS Earth Planet and Space 96 (2015).

[8] J. R. Eastman, IDRISI Selva Manual, Clark University, 2012.

[9] L. Martin-Fernandez, M. Marinez-Nuñez, An empirical approach to estimate soil erosion risk in spain, Science of the Total Environment 409 (2011) 31143123.

[10] L. Hui, C. Xiaoling, K. J. Lim, C. Xiaobin, M. Sagong, Assessment of Soil Erosion and Sediment Yield in Liao Watershed, Jiangxi Province, China, Using USLE, GIS, and RS, Journal of Earth Science 21 (2010) 941–953.
[11] H. Cramer, Mathematical Methods of Statistics, Princeton: Princeton University Press, 1946.
[12] B. S. Soares-Filho, G. C. Cerqueira, C. L. Pennachin, DINAMICA - a stochastic cellular automata model designed to simulate the landscape dynamics in an Amazonian colonization frontier, Ecological Modeling 154 (2002) 217–235.
[13] C. M. Almeida, M. Battyb, A. M. Vieira Monteiroa, G. Camaraa, B. S. Soares-Filhoc, G. C. Cerqueirac, C. L. Pennachind, Stochastic cellular automata modeling of urban land use dynamics: empirical development and estimation, Computers, Environment and Urban Systems 27 (2003) 481509.
[14] T. Wassenaar, P. Gerber, P. Verburg, M. Rosales, I. M., H. Steinfeld, Projecting land use changes in the Neotropics: The geography of pasture expansion into forest, Global Environmental Change 17 (2007) 86–104.
[15] R. G. Pontius, L. Schneider, Land-cover change model validation by an ROC method for the Ipswich watershed, Massachusetts, USA, Agriculture, Ecosystems and Environment 85 (2001) 239–248.
[16] R. G. Pontius, L. Schneider, Unplanned land clearing of Colombian rainforests: Spreading like disease?, Landscape and Urban Planning 77 (2006) 240–254.
[17] A. Comber, P. Fisher, C. Brunsdon, A. Khmag, Spatial analysis of remote sensing image classification accuracy, Remote Sensing of Environment 127 (2012) 237–246.
[18] V. Naipal, C. Reick, J. Pongratz, K. Van Oost, Improving the global applicability of the RUSLE model adjustment of the topographical and rainfall erosivity factors, Geoscientific Model Development 8 (2015) 2893–2913.
[19] V. Jetten, M. Maneta, Calibration of erosion models, in: M. R.P.C., N. M.A. (Eds.), Handbook of erosion modelling, Wiley Blackwell Publishing, 2011.
[20] J. Onyando, P. Kisoyan, M. Chemelil, Estimation of Potential Soil Erosion for River Perkerra Catchment in Kenya, Water Resources Management 19 (2005) 133–143.
[21] I. M. D. Rosa, D. Purves, C. J. Souza, R. M. Ewers, Predictive Modelling of Contagious Deforestation in the Brazilian Amazon, Plos One 8 (2013).

CAPITULO 4:

On the need of erosion control regulatory framework in Peru

On the need of erosion control regulatory framework in Peru (Spanish version)

Miluska A. Rosas

Graduate Student, School of Civil Engineering, Pontifical Catholic University of Peru

Abstract

La erosión de suelos es considerada como una fuente no puntual de contaminación de los cuerpos de agua, los gastos que puede generar a largo plazo son significativos y más aún en los países en desarrollo que no cuentan con un marco regulatorio como en el caso del Perú. Se han evaluado dos cuencas de gran interés nacional en términos de producción agrícola, interés industrial y económico, que son, la cuenca del río Santa y de río Jequetepeque. A partir de nuestro estudio se estimó una perdida $12.4 millones para la cuenca de Santa y $427 millones en la cuenca del Jequetepeque, causada por la pérdida de nutrientes para la actividad agrícola (on-site) y por la eliminación del volumen de sedimentos transportados hacia los cuerpos de agua (off-site). Si bien las costos son elevados, no se han considerado otros factores que también intervienen en el contexto de la cuenca. Nuestro estudio refleja la necesidad de un marco regulatorio en términos de erosión de suelos.

Keywords: erosión de suelos, GeoWEPP, contaminación no puntual, nutrientes, sedimentos

1. Introducción

Perú es un país en vías de desarrollo por lo tanto el aumento de áreas destinadas a actividades agrícolas, extracción de materia prima e infraestructura es inminente, estas actividades generan contaminación de fuentes no puntuales o difusas en los cuerpos de agua cuyas consecuencias son a largo plazo. La contaminación no puntual, a diferencia de las fuentes puntuales que son: vertimiento de desagües, plantas de tratamiento, industrias, etc; no ha sido un tema de interés en términos de contaminación ambiental y pérdidas económicas que esta genera [1]. Este tipo de contaminación no está limitado a un canal o tubería, sino que generalmente es causada por escorrentía, precipitación excesiva o filtraciones que transporta los contaminantes hacia los cuerpos de agua[2]. La erosión de suelos (ES) es considerada como una contaminación no puntual, y puede ser la fuente de cuantiosas pérdidas económicas, tanto para países desarrollados [3], como en vías de desarrollo, como es el caso de Zimbabwe ($117 millones) [4], Indonesia ($ 406 millones) [5] y Kenya ($ 390 millones) [6]. En el caso de la agricultura, el arrastre de sedimentos causa de la pérdida de nutrientes lo que implicaría costos adicionales en el uso de fertilizantes, el nuevo punto de equilibrio en la curva de oferta y demanda implica un aumento de precio y una disminución en la producción [7].

Las pérdidas económicas provocadas por la ES han sido clasificadas en dos grupos: on-site y off-site [8], la primera corresponde a pérdidas en el mismo lugar donde ocurre la erosión, como por ejemplo pérdidas de nutrientes, pérdida biológica-química, pérdida de producción. Las pérdidas

off-site se generan fuera del área de influencia del proceso de erosión, estos son: sedimentos en los cuerpos de agua, inundaciones, deslizamientos, deterioro de infraestructura, pérdida de en proceso de tratamiento de agua, entre otros.
Nuestro estudio, se basa en la cuantificación del gasto económico generado por la erosión de suelos en dos cuencas de interés nacional, que son, la cuenca del río Santa mediante la metodología RUSLE (Revised Universal Soil Loss Equation) y la cuenca del río Jequetepeque en donde se aplicó la plataforma GeoWEPP (Geo-spatial interface for Water Erosion Prediction Project), las cuales poseen un gran potencial agrícola y de generación de agua para consumo humano, con el objetivo de mostrar la necesidad de un marco regulatorio en términos de erosión de suelos para el Perú. La sección 2, muestra la metodología y los datos recolectados para realizar una cuantificación on-site (pérdida de nutrientes) y una off-site (sedimentos en cuerpos de agua) para la cuenca del río Santa y Jequetepeque, los resultados y una discusión de ellos se presentan en la sección 3 y la sección 4 muestra las conclusiones del estudio.

2. Datos y metodología

2.1. Erosión y producción de sedimentos en el río Santa

Muchos estudios han utilizado la ecuación de RUSLE para estimar la tasa de erosión en una cuenca determinada, esta sección muestra la metodología para su aplicación en el contexto de información limitada. RUSLE es matemáticamente definida por la Eq. 1.

$$A = R \times K \times L \times S \times C \times P \tag{1}$$

donde A es la erosión anual de suelos ($t\ ha^{-1}\ year^{-1}$); R es el factor de erosividad por precipitación ($MJ\ mm\ ha^{-1}\ h^{-1}\ year^{-1}$); K es el factor de erodabilidad de suelo ($t\ h\ MJ^{-1}\ mm^{-1}$); L el el factor de longitud de pendiente; S es el factor de pendiente; C es el factor de cobertura; y P es el factor de practicas de conservación (L, S, C y P son adimensionales) [9].

Para obtener el factor R, se aplicó la ecuación de Arnoldus (R_A, Ec. 2) y la de Renard and Freimund (R_{RF}, Ec.3). Estas relaciones fueron desarrolladas en diferentes contextos geográficos [10], sin embargo son comunmente usadas para estimar R en contextos donde no existe información detallada [11].

$$R_A = 0.264F^{1.50} \tag{2}$$

$$R_{RF} = 0.07397F^{1.847} \tag{3}$$

El factor K fue obtenido a través de la ecuación de Wishmer and Smith [12] que depende del contenido orgánico en el suelo (OM), el parámetro de tamaño de partícula (M), estructura de suelo (s) y permeabilidad (p). M se obtiene de la multiplicación de (% limo + % arena) by (100–$\%arcilla$). Por otro lado factores L y S fueron obtenidos con el modelo digital de elevación (DEM por sus siglas en inglés).
El factor C está basado en descripciones de cobertura vegetal y uso de suelo, y su influencia en la pérdida de suelo [12], y está matemáticamente definido por Ec. 4. Este factor envuelve el sub-factor de prior-land use (PLU), el sub-factor canopy-cover (CC), el sub-factor surface-cover (SC), el sub-factor surface-roughness (SR), y el sub-factor soil moisture (SM). Para mas detalles acerca de este factor, el lector puede referirse a [12].

$$C = PLU \times CC \times SC \times SR \times SM \tag{4}$$

El factor P representa las prácticas de conservación en áreas de cultivo y de pastoreo, con un rango de 0.0 a 1.0, y depende únicamente de s_c, la pendiente local en porcentaje. Los valores altos son asignados a áreas donde no se aplican prácticas conservativas [12].
Para más detalles del cálculo de cada factor y las fuentes de información para la estimación de la tasa de erosión en el Perú, se recomienda al lector remitirse a Rosas and Gutierrez [14] y [12].
La cuenca del río Santa descarga naturalmente al Océano Pacífico y según la Autoridad Nacional del Agua (ANA) es parte de la Unidad Hidrográfica 137 con un área de 11 596.5 Km^2 [13]. Se ubica entre los 7.9 y 10.2 de latitud sur y los 78.6 y 77.2 de longitud oeste, además comprende altitudes desde el nivel del mar hasta los 6768 msnm que correspondiente al Nevado Huascarán.
A partir del estudio de Rosas and Gutierrez [14], quienes construyeron el mapa de distribución espacial de erosión a escala nacional a una resolución de 5km, se ha obtenido el mapa de ES de la cuenca del río Santa (fig. 1.b). Respecto al punto de control ubicado a 8.65 latitud sur y 78.25 longitud oeste, presentando una tasa de ES de 5.24×10^6 Ton/año. Además con la metodología de Sediment Delivery Ratio [15] se presenta una tasa de sedimentos trasportados de 4.38×10^6 Ton/año.

2.2. Erosión y producción de sedimentos en el río Jequetepeque

WEPP es un software desarrollado por USDA-ARS con el fin de reemplazar las ecuaciones empíricas para estimar las tasas de erosión hídrica y transporte de sedimentos [16]. En proyecto WEPP se inició en el año 1985 y fue lanzado en el año 1989. El modelo realiza simulaciones de procesos físicos, tales como, erosión de suelos, escorrentía, transporte y acumulación de sedimentos a escala de cuenca y parcela para zonas de campos de cultivo, zonas de pastoreo, bosques y áreas urbanas. Ha sido aplicado con una alta aceptación tanto en los Estados Unidos [17] como al rededor del mundo [18]. El GeoWEPP se desarrolla con el fin de crear una herramienta que relacione las bondades del WEPP como modelo tradicional y la información geo-espacial [19], lo cual atiende la necesidad de los usuarios en términos de planificación de conservación de agua y suelo a escala espacial y temporal.
WEPP se basa en en tres grupos de información: información climatológica, data de elevación de superficie e información de tipo y uso de suelos; los cuales serán detallados brevemente a continuación, para mayor detalle de las ecuaciones involucradas en este modelo, sugerimos al lector remitirse a Ascough et al. [20] y Minkowski and Renschler [21].

Data meteorológica. GeoWEPP, además de presentar información de estaciones meteorológicas ubicadas en los Estados Unidos, cuenta con ciertas estaciones distribuidas en la superficie terrestre. Para nuestro caso, se ha considerado la data correspondiente a la estación Cajamarca (- 15.47 latitud sur, -71.92 longitud oeste y 8266 msnm de altitud) que se localiza en una región aledaña a la cuenca del río Jequetepeque. Esta información tiene una longitud de 14 años y comprende datos diarios de precipitación, temperatura máxima y mínima, viento, punto de rocío y radiación solar [21].

Data topográfica. Se recolecto información de ASTER Global Digital Elevation Model publicado por la Nasa y el Ministerio de Economía, Comercio e Industria de Japón, que provee data de elevación del 99% de la superficie terrestre a una resolución de 30 m de tamaño de pixel. Dicha información debe ser convertida a formato ASCII para ser leído por el modelo.

Uso y tipo de suelos. La base de datos para el uso de suelos fue Land Cover Share data, la cuál fue publicada por la FAO en el año 2014 y contiene la distribución espacial de 10 diferentes clases de uso de suelo. Respecto a la data de tipo de suelo se obtuvo a partir del mapa mundial taxonómico de suelos USDA publicado por el World Soil Information en el año 2014 a una resolución de 1km de tamaño de pixel.

La cuenca del río Jequetepeque descarga en la cuenca del Pacífico y abarca una extensión aproximada de 4 360 Km^2. Se ubica entre los 6.8 y 7.56 de latitud sur y los 78.36 y 78.7 de longitud oeste, además comprende altitudes desde el nivel del mar hasta los 4 000 msnm
Luego de incorporar la información de entrada al GeoWEPP, se obtuvo un mapa de distribución espacial de tasa de erosión a una resolución de 60 m de tamaño de pixel (ver figura 1.c), con un punto de control ubicado a -7.24 latitud sur y -73.15 longitud oeste. El modelo evaluó 448 subcuencas con un área mínima de 10 Km^2 (1000 Ha) y una longitud mínima de curso de agua de 100 m. La Tabla 1 muestra los resultados del modelo en la cuenca del río Jequetepeque, que muestran una tasa de ES promedio anual de 7.9×10^8 Ton/año y 2.6×10^8 Ton/año de transporte de sedimentos.

Table 1: Reultados del modelo GeoWEPP para la cuenca de río Jequetepeque

Total contributing area to outlet	322 075.39 ha
Avg. Ann. total hillslope soil loss	789 492 172.3 ton/yr
Avg. Ann. total channel soil loss	3 325 251 626.5 ton/yr
Avg. Ann. sediment discharge from outlet	260 264 164.0 ton/yr
Avg. Ann. Sed. delivery per unit area of watershed	808.1 Ton/ha/yr

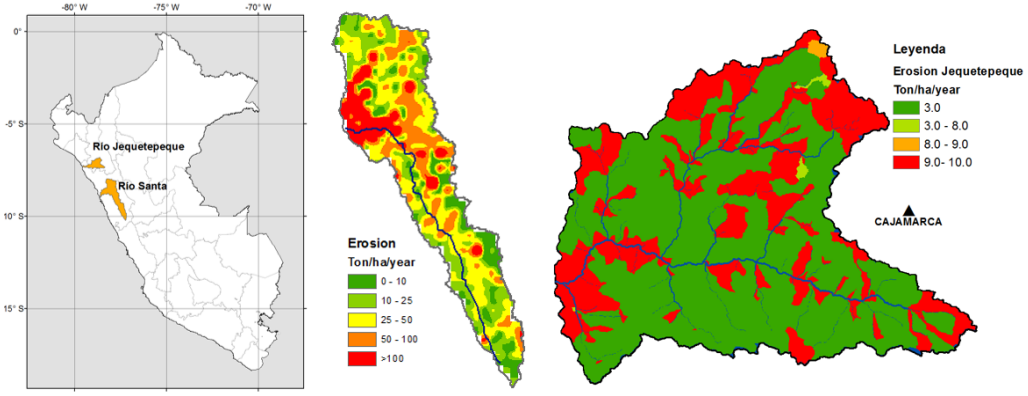

Figure 1: Mapas de erosión. (a) Mapa de ubicación de las cuencas del río Santa y Jequetepeque. (b) Mapa de erosión del río Santa en Ton/ha/año para el año 2010. (c) Mapa de erosión para el río Jequetepeque en Ton/ha/año.

2.3. On-site: pérdidas económicas por nutrientes

El cálculo se basa en la cuantificación de los nutrientes por tipo de suelo erosionado en la cuenca, luego, se le asignará el costo del fertilizante utilizado para reponer las pérdidas [22].

Los nutrientes evaluados serán potasio (K) y fósforo (P).
Se cuenta con el mapa peruano de capacidad de uso mayor (CUM) de suelos publicado por el Instituto Nacional de Recursos Naturales, las Tablas 2 y 3 muestra las características de cada clase en el área de interés.

Table 2: Capacidad de uso mayor (CUM) en la cuenca del río Santa. Cantidad de nutrientes y materia orgánica. La unidad ppm corresponde a 1mg de nutriente por kg de suelo.

CUM	Materia orgánica (%)	P (ppm)	K (ppm)
A2s (r)	1.4	12.8	256
A3se (r)	1.7	1.7	174
A3sec (r)	2.12	3.7	93
C3se	2.92	1.8	110
P2se	7.73	7.4	118
P2sec	7.73	7.4	118
P3se	2.18	2.0	2.91
P3sec	7.73	7.4	118
Xse	2.73	1.5	40
Xle	2.73	1.5	40

Table 3: Capacidad de uso mayor (CUM) en la cuenca del río Jequetepeque. Cantidad de nutrientes y materia orgánica. La unidad ppm corresponde a 1mg de nutriente por kg de suelo.

CUM	Materia orgánica (%)	P (ppm)	K (ppm)
A2s (r)	1.4	12.8	256
A3se (r)	1.7	1.7	174
A3sec (r)	2.12	3.7	93
F3se	4.49	4.7	37
P1s	7.73	7.4	118
P3se	2.18	2.0	2.91
P3sec	7.73	7.4	118
Xs	0.28	1.0	324
Xse	2.73	1.5	40
Xle	2.73	1.5	40

La clase y costo del fertilizante se obtuvo a partir del informe anual de precios de venta de fertilizantes publicado por la Gerencia regional de agricultura de la región de La Libertad, ubicada al norte de la cuenca evaluada, para el 2010. El fertilizante seleccionado es el Compuesto NPK (contiene 20% de nitrógeno, 20% de P y 20% de K) con un costo de S./89.5 la bolsa de 50 kg.

2.4. Off-site: pérdidas económicas por sedimentos en cuerpos de agua

El cálculo se basa en la cuantificación económica de las partidas de las obras civiles de remoción de sedimento y transporte hacia la escombrera o depósito [23]. A partir de costos actuales para actividades civiles, se ha considerado un valor de $\$1.35/m^3$ para la partida de remoción en terreno natural considerando un material estándar de excavación y un valor aproximado de $\$3.0/m^3$ por transporte y eliminación a escombrera para ambas cuencas.

3. Resultados y discusión

A partir de la base de datos mencionada se obtuvo el mapa de distribución espacial de cada nutriente en la cuenca del río Santa y Jequetepeque y los costos que estos representan (fig. 2 y 3).

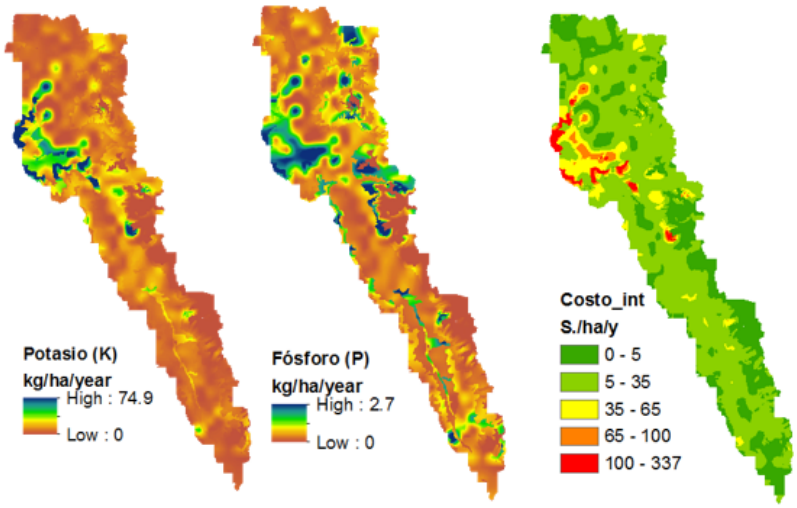

Figure 2: Costo inducido por pérdida de nutrientes, potasio (K) y fósforo (P) en S./ha/año para la cuenca de río Santa.

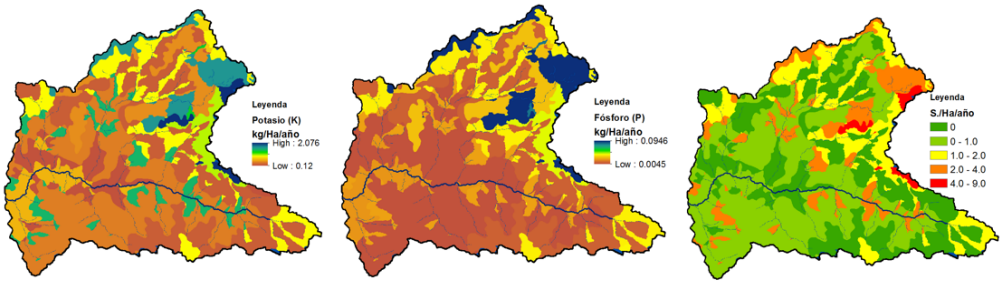

Figure 3: Costo inducido por pérdida de nutrientes, potasio (K) y fósforo (P) en S./ha/año para la cuenca de río Jequetepeque.

La tabla 4 presenta los costos estimados por pérdidas on-site y off-site para la cuenca del río Santa y Jequetepeque, dando un valor total aproximado de $12.4 y $427 millones al año respectivamente. El valor de la cuenca es muy elevado respecto al costo en la cuenca de río Santa, este efecto esta probablemente relacionado a la acción del Fenómeno El Niño que incide en la costa norte del Perú y por la existencia del reservorio de Gallito Ciego, localizado en dicha cuenca.

Table 4: Costos ambientales por erosión de suelos y arrastre de sedimentos.

Cuenca	Costo On-site $USD/año	Costo off-site $USD/año	Costo total $USD/año	Costo unitario $USD/ha
río Santa	5.2×10^6	7.2×10^6	12.4×10^6	11.9
río Jequetepeque	0.12×10^6	427.2×10^6	427.3×10^6	1288

4. Conclusiones

El estudio se ha basado en la estimación económica de ES por pérdidas de nutrientes y sedimentos en los cuerpos de agua, aún así es necesario realizar una estimación más detallada incluyendo factores y agentes adicionales que cumplen un papel importante en la cuenca de Santa, como por ejemplo infraestructura existente e industrias de potabilización de agua. Nuestros resultados reflejan la importancia de realizar un estudio a largo plazo que evalúe las pérdidas en los años futuros en las diferentes cuencas de nuestro país, de esta manera se considera urgente el desarrollo de un marco regulatorio que detenga el avance de los procesos erosivos como fuente de contaminación no puntual.

References

[1] M. O. Ribaudo, Non-point pollution regulation approaches in the us, in: J. Albiac, A. Dinar (Eds.), The Management of Water Quality and Irrigation Technologies, Earthscan, 2009.

[2] National Service Center for Environmental Publications, Protecting Water Quality from Agricultural Runoff Clean Water Is Everybody's Business, Technical Report, EPA United States Environment Protection Agency, USA, 2005.

[3] M. O. Ribaudo, Reducing Soil Erosion: Offsite Benefits, Technical Report 561, Natural Resource Economics Division, Economic Research Service, U.S. Department of Agriculture, Washington, D.C., 1986.

[4] M. Stocking, The Cost of soil erosion in Zimbabwe in terms of the loss of three major nutrients, Technical Report 3, FAO, Rome, 1986.

[5] W. Magrath, P. Arens, The costs of soil erosion on Java: A natural resource accounting approach, Technical Report 18, The World Bank, Washington, 1989.

[6] M. Cohen, M. Brown, S. K.D., Estimating the environmental costs of soil erosion at multiple scales in Kenya using emergy synthesis, Agric. Ecosyst. Environ. 114 (2006) 249–269.

[7] T. S. Telles, S. C. Falci Dechen, L. G. A. de Souza, M. d. F. Guimarães, Valuation and assessment of soil erosion costs, Scientia Agricola (2013) 209–216.

[8] T. S. Telles, M. d. F. Guimarães, S. C. Falci Dechen, The cost of soil erosion, R. Bras. Ci. Solo (2011) 287–298.

[9] V. Jetten, M. Maneta, Calibration of erosion models, in: M. R.P.C., N. M.A. (Eds.), Handbook of erosion modelling, Wiley Blackwell Publishing, 2011.

[10] K. G. Renard, J. R. Freimund, Using monthly precipitation data to estimate the R-factor in the revised USLE, Journal of Hydrology 157 (1994) 287–306.

[11] L. Hui, C. Xiaoling, K. J. Lim, C. Xiaobin, M. Sagong, Assessment of Soil Erosion and Sediment Yield in Liao Watershed, Jiangxi Province, China, Using USLE, GIS, and RS, Journal of Earth Science 21 (2010) 941–953.

[12] K. Renard, G. Foster, G. Weesies, D. McCool, D. Yoder, Predicting Soil Erosion by Water: A Guide to Conservation Planning with the Revised Universal Soil Loss Equation, United States Department of Agriculture, 1997.

[14] M. A. Rosas, R. R. Gutierrez, On a methodology to estimate hydraulic erosion rates in developing countries, Science of the Total Environment (2015).

[13] R. Villanueva, Características de la cuenca del río Santa, Unión Internacional para la Conservación de la Naturaleza (UICN SUR), Huaraz, Perú, 2011.

[15] J. Onyando, P. Kisoyan, M. Chemelil, Estimation of potential soil erosion for river perkerra catchment in kenya, Water Resources Management 19 (2005) 133–143.

[16] J. Laflen, W. Elliot, D. Flanagen, C. Meyer, N. M.A., WEPP - Predicting water erosion using a process-based model, Journal of Soil and Water Conservation 52 (1997) 96–102.

[17] C. S. Renschler, J. Harbor, Soil erosion assessment tools from point to regional scales - the role of geomorphologists in land management research and implementation, Geomorphology 47 (2002) 189 – 209.

192 [18] L. Pieri, M. Bittelli, J. Q. Wu, S. Dun, D. C. Flanagan, P. R. Pisa, F. Ventura, F. Salvatorelli, Using the Water Erosion
193 Prediction Project (WEPP) model to simulate field-observed runoff and erosion in the Apennines mountain range,
194 Italy, Journal of Hydrology 336 (2007) 84–97.
195 [19] C. S. Renschler, Designing geo-spatial interfaces to scale process models:the GeoWEPP approach, Hidrological
196 Processes 17 (2013) 1005–1017.
197 [20] J. Ascough, C. Baffaut, M. Nearing, B. Liu, The WEPP Watershed Model: Hydrology and Erosion, American
198 Society of Agricultural Engineers 40 (1997) 921 – 933.
199 [21] M. Minkowski, C. Renschler, GeoWEPP for ArcGIS 9.x Full Version Manual, Department of Geography The State
200 University of New York at Buffalo, New York, USA, 2009.
201 [22] L. Hein, Assessing the cost of land degradation: a case study for the Puentes catchment, southeast Spain, Land
202 Degradation and Development 18 (2007) 631–642.
203 [23] W. Rodrigues, Valoração econômica dos impactos ambientais de tecnologias de plantio em região de Cerrados., R.
204 Econ. Sociol. Rural 43 (2005) 135–153.